Some Applications of The Bioheat Equation in Hyperthermia

by

Robert Todd Constable

A thesis
presented to the University of Manitoba
in partial fulfillment of the
requirements for the degree of
Master of Science
in
Department of Physics

Winnipeg, Manitoba

ISBN 0-315-33997-7

SOME APPLICATIONS OF THE BIOHEAT EQUATION IN HYPERTHERMIA

BY

ROBERT TODD CONSTABLE

A thesis submitted to the Faculty of Graduate Studies of
the University of Manitoba in partial fulfillment of the requirements
of the degree of

MASTER OF SCIENCE

I hereby declare that I am the sole author of this thesis.

I authorize the University of Manitoba to lend this thesis to other institutions or individuals for the purpose of scholarly research.

Robert Todd Constable

I further authorize the University of Manitoba to reproduce this thesis by photocopying or by other means, in total or in part, at the request of other institutions or individuals for the purpose of scholarly research.

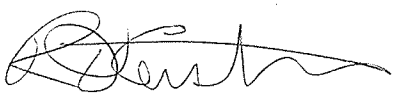

Robert Todd Constable

The University of Manitoba requires the signatures of all persons using or photocopying this thesis. Please sign below, and give address and date.

ABSTRACT

To date, satisfactory temperature monitoring during the clinical application of localized hyperthermia can only be achieved using invasive thermometry techniques. However, since the temperature can only be sampled at a limited number of locations using invasive thermometry, the temperatures in the majority of the tissue remain unknown. A mathematical model, the bioheat equation, which may be used to predict the resulting temperature distribution in a given tissue or tumor volume for a given Specific Absorption Rate distribution is presented. Finite difference techniques are then used to solve the governing partial differential equation.

The model is applied to study the self-heating of metallic thermometers under microwave irradiation and its effects on the steady-state temperature distribution. The results indicate that perturbations in the steady-state temperature distribution as great as 3 $^{\circ}$C may occur.

The model is further used to assess the thermal clearance technique for measuring blood perfusion levels. In addition, the consequences of the thermometer self-heating on thermal clearance measurements are investigated. It is shown that the calculated blood perfusion levels are susceptible to thermal conduction effects and that the characteristics of the thermometer probe play a significant role.

ACKNOWLEDGEMENTS

I wish to thank my supervisor Dr. P. Dunscombe for his guidance and support, Antonia Tsoukatos for many valuable discussions and entertaining coffee breaks and Dr. T. Lee for helping me wade through some of the math. I would also like to thank John McLellan and Ron Ellis for taking the time to proof read parts of this work and provide valuable suggestions. I must also thank programmers Lydia Bartel and Scott Cosby for their help.

The use of the facilities at the Manitoba Cancer Treatment and Research Foundation is acknowledged.

This work was funded in part by the Medical Research Council of Canada.

CONTENTS

Chapter I

INTRODUCTION

1.1 THE CANCER PROBLEM

Cancer is the second most common cause of death in North America.(1) It kills approximately 440,000 North Americans annually and its incidence appears to be increasing by approximately 2% each year. Forty years ago, fewer than 1 out of every 5 people diagnosed with cancer survived. Today 1 out of every 3 survives. Lung cancer is an exception in that its incidence and mortality is rising in both men and women. Cancer affects every age group, both sexes and every part of the body. More men die of cancer than women and more than half of all deaths occur after age 65. Most neoplasms appear to arise from a single cell that undergoes malignant transformation. If uncontrolled, cancer cells proliferate without organization and often without differentiation, invading normal tissues, disrupting body functions and eventually leading to the death of the host. The cancer may remain at the primary site or it may spread to other sites via blood or lymphatic routes.

1.2 CONVENTIONAL TREATMENTS

The management of cancer has changed dramatically during the past two decades. Treatment modalities have been refined to the point where each, alone, can produce positive results. However, the most important advance in cancer treatment has come from the realization that the best treatment is often some combination of the conventional modalities: surgery, radiation therapy and chemotherapy.(2,3) Local control of cancer is commonly attempted with surgery or radiation therapy. These techniques however, are not capable of controlling systemic disease to which purpose chemotherapy is applied.

While effective in the area of the primary tumor, surgery can do little for neoplasms outside the operative field. In addition, surgery cannot be performed on patients classified as high operative risks.

Ionizing radiations are effective in controlling a wide variety of malignant tumors and consequently they are used in the management of approximately two thirds of all patients with cancer. The application of radiation therapy seldom requires hospitalization or anesthetics and is less influenced by any concurrent medical problems the patient may have, all of which represent an advantage over surgery.

Chemotherapy is generally used for systemic control of cancer. In this modality, chemical reagents that have a specific and toxic effect upon the cancer are administered to the patient. Selective toxicity is possible primarily because of quantitative, not qualitative, differences between malignant and normal cells. Because of this, some degree of injury to normal tissues occurs. Fortunately, normal cells and cancer cells are not always equally vulnerable, though the margin of safety is often very narrow.

1.3 HYPERTHERMIA

The term HYPERTHERMIA (Greek;Hyper-above;Therme-heat) means elevated temperature and is biomedically employed to denote a febrile state as the result of thermotherapy. The attempt to exploit elevated temperatures to control malignant tumors has a history longer than the use of ionizing radiations and can be traced to 400 B.C., as recorded in the writings of Hypocrates.(4)

The recent renewal of a strong interest in the use of Hyperthermia for the treatment of malignant disease is likely to last as it is based on documented clinical evidence of tumor regression and on encouraging results from extensive laboratory experiments with both in-vivo and in-vitro systems. It is known that exposure of malignant

cells to temperatures between 42 and 45 ^{o}C may retard or totally inhibit their growth. Similarly heated normal cells will also suffer damage or destruction, but their net sensitivity appears to be less pronounced and a larger cell fraction will survive.

While localized hyperthermia can induce regressions in human neoplasms by itself, superior results can be obtained by integrating hyperthermia with chemotherapy or radiotherapy.(2,5,6) This combination of heat and ionizing radiation or chemotherapeutic agents can allow for reduced dosage requirements to effect a particular response to treatment.(7) Several clinical trials have demonstrated that hyperthermia, as an adjuvant to radiation therapy, can produce higher tumor response rates than the same irradiation alone while minimal enhancement of irradiation effects on normal tissues have been reported.(8)

The effectiveness of hyperthermia depends both on the ability to raise the temperature of the tumor-bearing tissue and to maintain it at a certain level for a period of time while sparing any normal tissue from excessive heat damage. The difficult part of this treatment is, predictably, the delivery of well controlled heat into the body, a complex biological system.

1.4 BIOLOGICAL BASIS

Hyperthermia is useful in combination with radiotherapy for many reasons. First, it has been shown that heat interacts synergistically with radiation. Those cells that are the most resistant to radiation, S-phase cells in the DNA synthetic phase, are the most sensitive to heat. In addition radioresistant hypoxic cells are believed to be at least as sensitive to heat as radiosensitive oxygenated cells.

Furthermore, experiments have indicated that nutritionally deprived cells, which probably exist in many tumors, are more sensitive to heat than adequately fed cells. It is commonly thought(11) that heat may be more damaging at low pH, and as tumors tend to be acidic due to anaerobic metabolism, they should be preferentially more sensitive to heat than normal tissue. It is also possible that neoplastic cells may be intrinsically more sensitive to heat than normal cells.

Finally, heat has been shown to prevent the repair of potentially lethal damage(PLD) from x-rays. Since the repair of PLD is observed in irradiated tumors (probably in the nutritionally deficient cells) but presumably does not occur in normal cells, heat would be expected to be selective in potentiating the radiation response of the tumor.

1.5 PHYSIOLOGICAL CONSIDERATIONS

1.5.1 Tumor Vasculature and Differential Heating

One of the most critical effects to be considered in the planning, application and assessment of a hyperthermia treatment is the effect of blood flow. Blood flow plays a major role in heat dissipation especially in large well perfused tissue masses, and can have a profound effect on the outcome of a treatment. As well, the growth and continued expansion of a tumor depend upon the development of neovasculature which differs from normal vasculature in various ways.

Tumor vasculature develops from preexisting normal vessels and morphologically resembles large tortuous capillaries. It is often irregular with substantial regional variations in blood flow throughout the tumor. In addition, hypovascularized regions within a tumor are not uncommon. Normal tissue perfusion rates however also vary substantially and are organ or tissue type dependent.

Generally tumor blood flow rates lie between those of resting peripheral tissues and several highly perfused organs. Blood flow in muscle and skin however, increases markedly with temperature. In addition, tumor vasculature is more vulnerable to heat damage than the vascular beds in normal tissue.(9) This increase in blood flow in human skin, muscle and fat, coupled with the decrease in blood flow in

tumor tissue as a result of vascular damage, may permit the differential heating of some tumors or tumor regions when heat is deposited equally in tumor and normal tissue. Thus effective differential heating occurs when the blood flow of any overlying and adjacent normal tissue is greater than the flow in tumor tissue even if the energy is deposited uniformly in both tissues. Generally however, variations in blood flow within tumors and at the normal tissue/ tumor tissue margin will preclude uniform tumor heating. It has been shown that small differences in tissue temperature may be expected to have a major impact on tissue response to hyperthermia.(10) This is one reason why hyperthermia will be most effectively applied in combination with other forms of therapy.

1.5.2 pH and Thermal Sensitivity

The second major rational for hyperthermia in cancer therapy is based on the low pH of tumors compared to normal tissues, as mentioned above. It is an established fact that an acidic environment greatly increases thermal damage.(11) The microenvironment in malignant tumors is intrinsically acidic relative to normal tissue probably due to the elevated level of glycotic metabolism accompanied by the formation of lactic acid. Lactic acid formation is increased due to an enhanced metabolic rate without a concomitant increase in the oxygen supply. Low blood flow

resulting from vascular damage by heat then leads to insufficient drainage of the lactic acid resulting in sustained depression of the pH.

Many studies have demonstrated that although regional variations exist the average and extreme extracellular pH values are lower in tumor than in normal tissue.(9) Generally, the larger the tumor the more acidic it will be. Song(11) has shown that hyperthermia itself triggers an immediate and significant decrease in pH in tumors. Thus pH tends to decrease as more hyperthermia sessions are administered. Studies have shown that a reduction in the pH of the extracellular medium below 7.0 results in a marked reduction in the fraction of cells surviving heat treatment at 42 ^{o}C.(10)

In general, the magnitude of the pH sensitivity effects is most pronounced in the 41-43 ^{o}C temperature range and decreases at higher temperatures. There are indications that in addition to enhancing the heat killing directly, acidic conditions also inhibit the repair of thermal damage and the development of thermal tolerance.(12) The decrease in intratumor pH by heat may therefore have a profound effect on the thermal damage on tumor cells in vivo. Goldin(13) showed that decreased extracellular pH (<7.0) reduced the development of thermotolerance and reduced recovery from potentially lethal hyperthermia damage. pH

also plays an important role in the inhibition of thermotolerance induction as will be discussed below.

1.5.3 Oxygen Content

A vitally important difference between x-ray therapy and hyperthermia treatment is the response of hypoxic cells to the two modalities. Hypoxia protects cells from the killing effect of x-rays. By contrast, hypoxic cells are not more resistant than aerobic cells to hyperthermia and evidence suggests that they are slightly more sensitive.(14) This increased sensitivity of hypoxic cells relative to aerobic cells is not due to hypoxia per se but is a consequence of the lowered pH or the nutritional deficiency that cells suffer as a result of hypoxia. Cells nutritionally deprived or at a decreased pH are likely more sensitive to heat even when aerobic. Since these suboptimal conditions often apply to tumors, where hypoxic cells may be deprived of nutrients due to an over stretched vascular supply and may be in a low pH environment due to an accumulation of lactic acid, it may be that hypoxic tumor cells in vivo are also particularly vulnerable to killing by heat. Decreased oxygen tension in the smooth muscle of blood vessels and in the parenchymal cells, lacking in tumor vasculature, causes vasodilation and opening of more capillaries resulting in increased blood flow through normal tissue. Since tumor vasculature cannot respond in this way, this may lead to differential heating of the tumor versus normal tissue as discussed earlier.

1.5.4 Nutrient Availability

Under conditions of extreme nutrient deprivation cell death occurs rapidly at 37 °C. Nutrient deprivation probably gives rise to the necrotic foci which are observed in tumors as the radial distance from functioning capillaries increases. Between the nutrient rich capillaries and the necrotic zone lie viable cells within a gradient of decreasing oxygen and glucose concentration. The presence or absence of either oxygen or glucose alone has little effect on the thermal sensitivity.(15) However, when the supply of both nutrients is sufficiently reduced to bring about a reduction in intracellular adenosine triphosphate (ATP) levels, thermal sensitivity is enhanced markedly. Thus it is not nutrient concentration alone but the effect of nutrient level on the intracellular ATP concentration that affects thermal sensitivity. Nutrient availability and pH are closely related to one another in terms of their effect on tissue sensitivity to heat. Modification of thermal sensitivity by nutrient availability is dependent upon pH. The greatest effect occurs at an alkaline pH and the effect is minimized as the pH is reduced.

1.5.5 Thermotolerance

Thermotolerance is defined, for temperatures above 43 °C, as the resistance to a second heat dose following an initial

heat challenge and incubation at 37 ^{o}C.(14) The greater sensitivity of cells at low pH, the reduced thermal resistance at low pH and the possibly reduced capacity to accumulate sublethal damage (SLD) all imply that a fractionated therapy regimen may be improved by selecting intervals that allow normal tissue maximal opportunity to develop thermotolerance.

Thermotolerance is not permanent but it does persist for some time after the cells are returned to 37 ^{o}C. The degree of thermotolerance is dependent on the magnitude of the first treatment, with respect to both temperature and duration of treatment. The time required for the development of maximum thermotolerance also varies with the magnitude of the initial heat treatment from a few hours, following a very mild initial treatment to 10 to 15 hours following a severe initial treatment. The effects may still be apparent several days later, significantly modifying the cellular response to a second treatment. Thus a knowledge of tissue tolerance decay kinetics could be of substantial assistance in designing hyperthermia fractionation protocols which minimize damage to heated normal tissues while maximizing damage to tumor tissue.(16) Note that this is quite different from the repair observed with x-rays; the repair of SLD following an exposure to x-rays is complete within approximately two hours.

1.6 TECHNIQUES OF HEAT DELIVERY

The delivery of energy to tumors without unacceptable normal tissue heating is a necessary prerequisite for the clinical application of hyperthermia. The methods used for clinical hyperthermia can be divided into three areas: local, focal and whole-body techniques.

In local, energy from some externally placed electromagnetic(EM) or ultrasound(US) power source is deposited in a large volume which includes the tumor and reliance is placed on the existence of differential properties of the tumor to cause its temperature to rise higher than that of the neighboring normal tissues. For this reason precise knowledge of tumor location and geometry is not important.

In contrast, focal techniques deposit energy directly in the tumor volume. Thus less reliance is placed upon special tumor properties with the requirement that the energy must be directed precisely at the tumor.

In whole-body hyperthermia the entire body is raised to a minimally therapeutic temperature. This work will deal primarily with electromagnetic local heating techniques as described below.

1.6.1 Electromagnetic Techniques

Electromagnetic techniques are commonly used to heat superficial tumors and those located at a few centimeters depth. Microwaves have an advantage over US in that they are not hindered by bones and are particularly useful for applications involving lung tissues because of the lower attenuation in air and hence better penetration.(17) Electromagnetic heating then, is the method of choice in areas such as the lungs, stomach, bowel, bladder, rectum and pelvis due to the presence of air.(17) Also, since EM energy is not hindered by bones it can be used in the chest area and all portions of the upper and lower extremities. However, a depth of penetration greater than a few centimeters is generally difficult to attain although forced surface cooling can aid in increasing the depth of penetration. The frequency of the incident EM wave also has an effect on the depth of penetration. An increase in the frequency of the wave usually leads to a decrease in the depth of penetration. Because of this frequency dependence, to heat tumors at various depths it is desirable to have a generator which covers a range of bandwidths. For hyperthermia the EM generators that are commercially available operate at frequencies of 13.56, 27.12, 40.68, 915 and 2450 MHz. A frequency of 433 MHz is also authorized in Europe.

The power range used in hyperthermia also varies, normally within a range of 10 to 500 Watts for a single applicator at microwave frequencies of 915 and 2450 MHz. The calculations performed in this work are for 2450 MHz waves. As focusing is very difficult with microwaves, particularly at the lower frequencies needed for adequate penetration, focal methods are not widely used.

While microwaves have many desirable characteristics in terms of their heating ability, interaction of EM radiation with metallic temperature monitoring devices is possible and this can lead to difficulties in monitoring the temperature. This problem is discussed in detail in Chapter 4. Another disadvantage in using EM radiation is that large reflections can occur at the fat/muscle interfaces possibly generating standing waves in the subcutaneous fat layer thus creating hot spots.

1.6.1.1 Interaction of EM-Waves with Materials

Materials are composed of atoms made up of positively and negatively charged particles. When an electric or magnetic field is impressed upon a material it exerts forces on these charged particles causing them to undergo displacements or rearrangements to modify the incident fields. Since tissue is a nonmagnetic material, there are only three basic mechanisms that can describe its interaction with EM waves.

These include: displacement or drift of the conduction(free) electrons and ions in the tissue; polarization of atoms and molecules to produce dipole moments; orientation of the already existing dipoles in the direction of the applied E-field.

Generally, the heat produced by the absorbed power is related to the orientational friction associated with the vibration of atoms and molecules in the time-varying fields as well as the collisions of the free conducting electrons with other atoms and molecules. At microwave frequencies(300MHz to 30GHz)the rotation of water molecules dominates all other interactions; therefore water-containing tissues like skin and muscle are usually good microwave absorbers.

1.6.2 Ultrasound

Ultrasound, while not dealt with directly in this work, deserves mention here as it is a commonly used method of producing deep heating in hyperthermia cancer therapy. Its primary advantage is its large depth of penetration and the ease with which the US waves can be focused. Vibration due to the passage of ultrasound waves through tissues causes the displacement of the tissues molecules. Heating is produced as a result of the absorption of this vibrational energy in the tissue.

The speed of sound in tissue is much lower than the velocity of EM wave propagation. This difference in velocities and differences in the US and EM radiation results in vast differences between ultrasonic and EM heating. Because of the relatively low speed of sound in tissue (1.5x10**5 cm/sec) at frequencies between 1 and 10 MHz the acoustical wave lengths (between 1.5 to 0.15 mm) are much shorter than those in the EM range. This frequency range is still high enough however to avoid excessive tissue absorption and as a result provides deep penetration in tissue.

Propagation of US in the body is similar to that of microwave beams. The acoustic impedance Zx is related to the velocity of ultrasound V (speed of sound in region x in m/sec) and the average density of tissue Px (kg/m3) by the equation Zx=Px*V . At ultrasound frequencies both the speed of sound and the average density are almost constant for most tissues, except bone, and as a result the acoustic impedance Zx is constant for different tissues. Because of this, internal reflections between fat and muscle are usually neglected. However propagation of US waves in bone and air differs markedly from that of soft tissue due to acoustic impedance mismatch and as a result a great deal of reflection occurs at interfaces with these surfaces. This is a major disadvantage with the ultrasound technique. Due to difficulties encountered in monitoring temperatures,

especially at depth, the majority of tumors treated today are close to the surface where microwaves are most efficient at heating.

1.6.3 Capacitively Coupled RF or Microwave Electrodes

Capacitively coupled radiofrequency or microwave electrodes are simple devices which operate at low frequencies (10KHz to 300MHz). In the capacitive mode, either RF or microwave current, passes from one electrode to another through tissue interposed between a set of electrodes. The shape of the heated region can be controlled to some extent by the electrode configuration.(18,19) Unfortunately, excessive heating of the fat layer, at fat/muscle interfaces, is often a problem with this method of heating. In addition, burns may occur along the edge of the electrodes due to the high current density there.

1.6.4 Multiple-Applicator Focused Heating Techniques

Electromagnetic focused heating techniques or phased arrays, can deposit power at depth relatively uniformly. However this does not necessarily lead to adequate or even predictable temperature distributions in deep seated tumors.(20,21) The units are very complicated to operate due in part to the difficulty of predicting the specific

absorption rate pattern in a given patient. Furthermore, energy coupling is very sensitive to the load and operating frequency, and must be adjusted for each patient.(22) Focused US heating techniques with plane wave transducers have also been used for cancer therapy and are capable of delivering highly focused energy to deep seated tissue volumes.(21) However, as discussed earlier, ultrasound waves do not propagate through air cavities and are reflected and absorbed by bone thus limiting their use to only a select number of sites.

1.6.5 Interstitial Techniques

Interstitial techniques have been used for producing controlled temperatures in small volumes.(22) With these techniques the ability to heat the proper volume is not in question, the major concern is the invasive nature of the procedure and the surgical requirements. Interstitial techniques include:

1. localized current fields
2. microwaves radiated from needle dipoles
3. finite sized ferromagnetic implants
4. injected ferromagnetic fluids.

Care must be taken with interstitial techniques as metastasis caused by delivering heat invasively might increase with the disruption of blood vessels and mechanical probing of the tumor.

1.6.6 Whole-Body Hyperthermia

The same methods applicable for inducing regional hyperthermia can also be used to induce systemic hyperthermia.(23) Hot water/wax baths have also been used as well as a method which extracts the blood and circulates it through a heat exchanger before returning it to the patient. Historically whole-body hyperthermia has been used in combination with chemotherapy as a systemic therapy against metastatic disease rather than with radiotherapy to treat localized tumors.(7)

1.7 THERMAL DOSIMETRY AND THERMOMETRY

Some quantitative criteria for characterizing thermal treatments is required to allow a valid comparison of clinical trials. To date, a satisfactory definition of thermal dose has not been developed. The conventional method of determining the dose, by using the energy deposited per gram of tissue, as in radiation studies, is not suitable for hyperthermia as the heat damage is not dependent on the power deposited but on the temperature achieved and the time that temperature is maintained.

A nonlinear relationship exists between temperature and heating time. The relationship undergoes a transition in the 42 to 43 ^{o}C temperature range above which, a change in temperature of 1 ^{o}C is equivalent to a change in heating time

by a factor of two, to produce the same level of damage. Below this transition point a change of 1°C is equivalent to a change in heating time by a factor of four to six.(24)

Many definitions of thermal dose have been discussed in the past.(25) The most widely accepted is that which relates treatments at various times and temperatures to equivalent times at 43°C. This method involves converting all thermal exposures during a treatment to equivalent minutes at a temperature of 43°C.(26,27,28)

As is obvious from the above discussion, any attempt to define a thermal dose accurately is highly dependent on the ability to measure temperatures accurately. It is also evident that for effective clinical application of a hyperthermia treatment, a well controlled heating field must be produced. The object of this work is to present a model that can be used to predict the history of the instantaneous temperature distribution and/or the fixed temperature pattern within a thermally conducting body exposed to a different temperature environment. The model is presented in Chapter 2. In practice there are a number of complications, including problems of realistically specifying boundary conditions, the necessity to handle complicated body geometry and the associated problems encountered when dealing with nonhomogeneous tissues. These issues are also discussed in Chapter 2. Finite difference

equations for the numerical solution of the governing partial differential equation describing the heat transfer mechanisms involved, are derived in Chapter 3. In Chapter 4, the model is applied to evaluate the effect of self-heating of metallic thermometers, under microwave irradiation, on the steady-state temperature distribution. The consequences of the time dependence of the local temperature perturbations on thermal clearance methods for measuring tissue blood perfusion are investigated in Chapter 5.

1.8 REFERENCES

1. American Cancer Society.A Cancer Source Book For Nurses, Professional Education Publication.New York,1981.

2. Perez C.A.,In Physical Aspects of Hyperthermia.AAPM Medical Physics Monograph No.8.p.63-89.1982

3. Haskell C.M.,Cancer Treatment,2nd ed.,W.B.Saunders Company, Philadelphia,1985

4. Nauts H.C.,In Proceedings of the International Symposium on Cancer Therapy by Hyperthermia and Radiation.Washington D.C., American College of Radiology.p.239-250,1975

5. Fairman H.D., Journal of Laryngology and Otology, 96,251-263,1982

6. Vaeth J.M.(ed),Frontiers of Radiation Therapy and Oncology vol.18.Hyperthermia and Radiation Therapy/Chemotherapy in The Treatment of Cancer,1983.

7. Kowal C.D., Bertino J.R., Cancer Research 39,2285-2289,1979

8. Meyer J.L.,Cancer Research(suppl.)44,4745s-4751s,1984

9. Song C.W.,In Physical Aspects of Hyperthermia,AAPM Monograph No.8,p.43-62,1982

10. Gerweck L.E.,Cancer Research 45,3408-3414,1985

11. Song C.W.,Radiology 137,795-803,1980

12. Goldin E.M.,Radiology,141,505-508,1981

13. Goldin E.M., Leeper D.B., Radiation Research 85,472-479,1981

14. Hall E.J., Radiobiology for the Radiologist.2nd ed., Harper and Row, Philadelphia,325-348,1978

15. Gerweck L.E.,Radiation Research 99,573-581,1984

16. Urano M., Kahn J., Int. J. Rad. Oncol. Biol. Phys., 12,89-73,1986

17. Cheung A.Y., Neyzari A., Cancer Research (suppl.)44,4736s-4744s,1984

18. Brezovich E.V., Int. J. Rad. Oncol. Biol. Phys., 7,423-430,1981

19. Oleson J.R.,IEEE Trans.Bio.Eng.,BME-31,91-97,1984

20. Gibbs F.A.,IEEE Trans.Bio.Eng.,BME_31,115-119,1984

21. LeLe P.P., Hyperthermia in Cancer Therapy. Strom (ed), 333-367,1983

22. Cetas T.C., Roemer R.B., Cancer Research (suppl.) 44,4894s-4901s,1984

23. Milligan A.J., Cancer Research (suppl.) 44,4869s-4872s,1984

24. Overgaard J., Suit H.D., Cancer Research 39,3248-3253,1979

25. Sathiaseelan V.,et al,British Journal of Radiology 58,1187-1195,1985

26. Dewhirst M.W., Sim D.A., Cancer Research (suppl.) 44,4772s-4780s,1984

27. Perez C.A., Sapareto S.A., Cancer Research (suppl.) 44,4818s-4825s, 1984

28. Sapareto S.A., Dewey W.C., Int. J. Rad. Oncol. Biol. Phys., 10,787-800,1984

Chapter II

HEAT TRANSFER MECHANISMS IN A BODY

2.1 HEAT TRANSFER CALCULATIONS

The successful application of local hyperthermia as a modality for the treatment of cancer depends upon the ability of the clinician to deliver heat locally and monitor the temperature accurately. A well defined temperature distribution in a carefully delineated volume of tissue that encompasses the tumor, must be produced. However, one of the more difficult problems in clinical hyperthermia is the determination of the complete temperature field throughout both the tumor and normal tissues. Ideally, a hyperthermia system would allow the clinician to heat and measure the temperature distribution of the tumor and surrounding normal tissue noninvasively and in 3-Dimensions. Theoretically a number of techniques (CT-scanning etc.(1)) promise noninvasive 3-D temperature measurement; however it is expected to be sometime before these systems become available for practical use. Thus for now at least, invasive temperature probes must be relied upon to quantify the temperature elevation at a limited number of sites from which the temperature field in the remaining tumor and host

tissue can be estimated. Since temperatures can be sampled only at a limited number of locations during clinical heating the temperatures in the majority of the tissue remain unknown and it is therefore difficult to assess the efficacy of the treatment protocol utilized.

The physics requirement is to predict the resulting temperature distribution in a given target volume for a given Specific Absorption Rate (SAR) distribution. As the objective of hyperthermia is to damage tumor tissue with heat, the design of these modalities depends strongly upon an understanding of the ways in which tissue (neoplastic and normal) is able to respond to energy inputs in the form of heat. The successful estimation of the temperature field requires a mathematical model that incorporates the patient anatomy, the power deposition pattern in the heated tissue, the physiological response of the patient and the thermal interactions in the tissue.(2) The idealization of this is usually in the form of a partial differential equation for the temperature of the material as a function of space and time. The heat transfer mechanisms that lead to this equation, called the bioheat equation, as discussed by Bowman(3), are presented below.

2.2 THE BIOHEAT EQUATION

There are five heat transfer mechanisms in tissue which are of interest. These include: tissue conduction, metabolic heat generation, storage of thermal energy,convection (heat transfer via the vascular architecture and perfusion rate) and energy absorbed from external sources.(3,4,5) The interactions of these individual mechanisms within a tissue volume may be visualized by considering the control volume shown in Figure(2.1).

The control volume maintains thermal contact with the surrounding tissue by heat conduction and blood flow across the surface. For the control volume to remain in equilibrium with the surrounding tissue, any heat generated within the volume through metabolism and by the absorption from external sources must be transferred to adjacent tissue by conduction, transported by the blood stream or stored internally where it results in a change in temperature of the control volume. It should be noted that human tissues are difficult materials to describe analytically because of their nonhomogeneous anisotropic and generally highly complex composition, structure and function.(3)

2.2.1 Tissue Conduction

Fourier's law of heat conduction, which states that the heat flux is proportional to the temperature gradient dT/dxi where the proportionality constant is defined as the thermal conductivity kij, governs the convective heat flux vector qi, such that

$$qi = - kij \frac{dT}{dxj} \qquad ...(2.1)$$

Where, i and j are nodal points on orthogonal axes. The negative sign is required by the second law of thermodynamics so that the heat flux is in the direction of decreasing temperature.

In general, Fourier's law has certain limitations and some important points must be considered when it is implemented; these include

1. If the thermal conductivity is not constant--then it holds only roughly over small intervals Δx ;
2. If the thermal conductivity is direction dependent--then the k appropriate to the direction being considered must be used.

Thus the thermal conductivity determines the temperature gradient for a given steady-state heat flux. In this work, Kij is assumed to be independent of direction and temperature. However, it should be note that in many cases Kij is often both temperature and position dependent due to the complex structure of tissue.

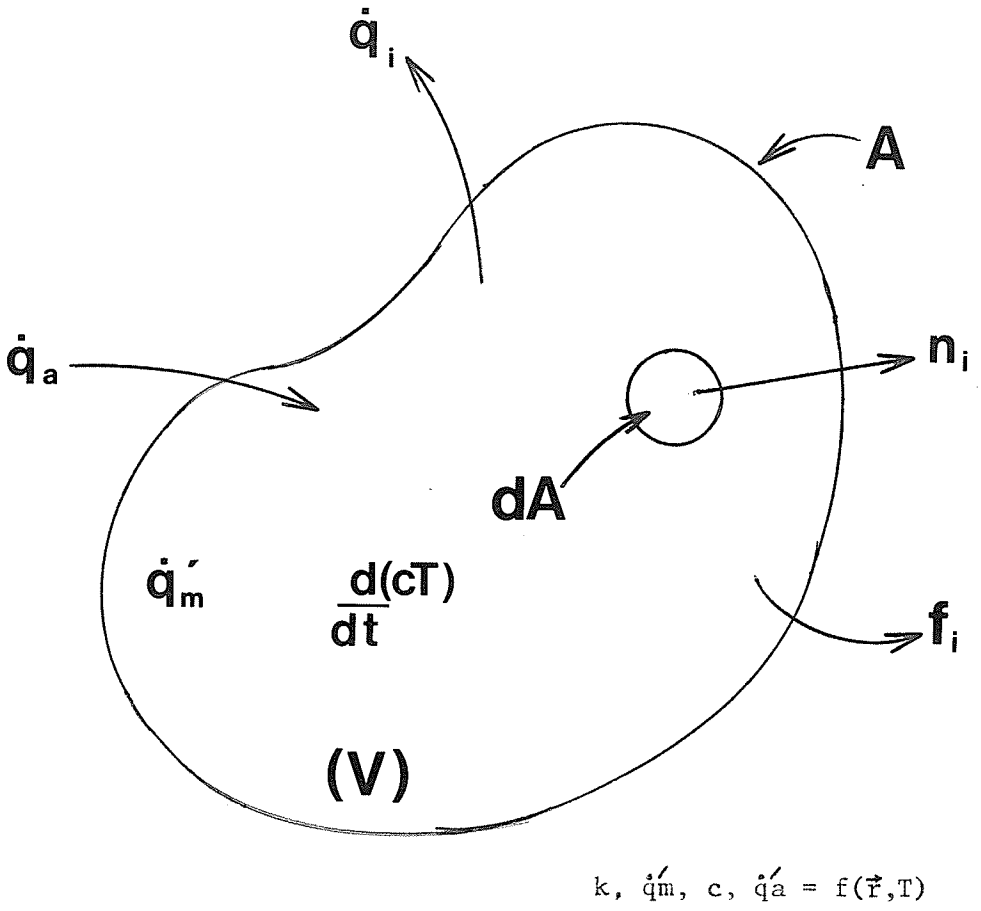

Figure 2.1

Control volume representing the five mechanisms of heat transfer: conduction, metabolic heat generation, storage of heat energy, convection and energy absorbed from an external source.

From: Bowman ref.3.

Integration of the conduction heat flux vector qi over the control surface yields the total heat conduction $\mathring{q}c$. Thus we have

$$\mathring{q}c = \int_A kij \frac{dT}{dxj} ni \, dA \qquad ...(2.2)$$

Note that the thermal diffusivity $\alpha = k/pc$, describes the transient heat conduction, where p is the tissue density and c is the specific heat. This defines the ability of a thermally perturbed medium to relax back to the steady-state conditions.

2.2.2 Metabolic Heat Generation

Heat is generated by all tissues as a consequence of aerobic or anaerobic metabolic processes.(3) Generally, the tissue base-line temperature is determined by the level of metabolic heating and heat loss. While this is not a mechanism of critical importance in heat transfer calculations for the application of hyperthermia it is included to satisfy the overall heat balance. Jain has shown that changes in temperature due to the metabolic rate are small and hence the term Qm can often be neglected.(6)

By integrating the heat production rate $\mathring{q}'m$, which is often both temperature and flow dependent, over the control volume, the total metabolic heat generated can be determined. Thus we can write

$$\dot{q}_m = \int_V \dot{q}'_m \, dV \qquad \ldots(2.3)$$

The metabolic heat production term has been neglected in the following chapters. However, it is indirectly accounted for in the initial temperature distribution.

2.2.3 Energy Storage

Temperature is a measure of the amount of energy stored per unit mass within a medium.(3) The amount of stored energy is changed when the rate of energy produced in the control volume does not equal the rate of energy removed from the control volume. This imbalance results in a change in temperature of the control volume. The time derivative of the volume integral of the product (pcT), where the specific heat, c, is a function of temperature (in some cases) and of position (when there are changes in composition), yields the rate of change of stored thermal energy $\dot{q}_s$. Thus in integral form we have

$$\dot{q}_s = \frac{d}{dt} \int_V pcT \, dV \qquad \ldots(2.4)$$

2.2.4 Thermal Transport(convection)by the Vascular Network

Convective heat transfer takes place when whole groups of molecules carry heat from one place to another. From Chapter 1 it is clear that the vascular system, through vasoconstriction and vasodilation, plays an important part in temperature regulation. Thermal convection in tissue is characterized by the geometrical organization of the vascular bed and the blood flow rate which is also subject to thermal regulation. For an exact solution involving blood flow one would need:

1. a complete description of the anatomy of all blood vessels in the region of interest.(i.e./diameter, length and positions of all arteries, veins, capillaries, venules and arterioles)
2. a complete description of the type of flow and the velocity field within each of these vessels.(8)

It is apparent that the large number of vessels of widely varying dimensions can make different contributions in the overall heat transfer process. Integration of the product of $cb \cdot Tb \circ fi$ over the control surface yields the net thermal energy $\dot{q}b$, transported by the blood vessels across the control surface, where cb and Tb are the specific heat and temperature of the blood and fi is the blood perfusion rate vector. This mass flux vector fi, is set to zero everywhere on the surface except where there are blood vessels in which case it then has a value specific to that vessel.

$$\dot{q}b = \int_A cb \cdot Tb \cdot fi \cdot ni \; dA \qquad \ldots(2.5)$$

This equation however is impractical in its use as most of the information required is unavailable at this time. In addition the computational task would be horrendous.

The types of tube flow situations for which complete analytical solutions are available are mainly those for laminar flow of simple fluids in regular geometric channels (eg. circular tubes). For the case of pulsatile flow, through irregular vessels, of two-phase blood (solid and liquid components), the additional difficulties are obvious. Therefore some approximations are needed.

Pennes(7), in 1948, was the first person to deal with this problem. He reasoned that the capillary bed, in the absence of large vessels, is the major site of heat exchange between tissue and blood and that venous blood leaves the tissue at the tissue temperature. He expressed the volumetric rate of blood tissue heat exchange, $\dot{q}'b$, in terms of a tissue average volumetric perfusion rate, wb.(3) That is:

$$\dot{q}'b = wb \cdot cb \cdot (Ta - Tv) = wb \cdot cb \cdot (Ta - T) \qquad \ldots(2.6)$$

where cb is the specific heat of blood and Ta, Tv and T are the arterial, venous and tissue temperatures, respectively. This term assumes that the blood enters the control volume

at the arterial temperature Tb, comes to equilibrium at the tissue temperature T, and then carries away energy as it leaves the control volume hence acting as a heat sink when Tb < T.

The assumption implies that arterial blood reaches any two points within the tissue with the same arterial blood temperature Ta regardless of the difference in distances which separate the two points from the arterial supply vessel. However this is not physically realistic. It should also be noted that this blood perfusion term is a scaler and thus fails to account for the vectoral character of thermal convection due to blood flow. The perfusion term has thus been obtained from the energy balance for the blood in the entire domain, D, and then applied to the local tissue energy balance for an infinitesmal control volume.

2.2.5 Energy Absorbed From An External Source

Three modalities are commonly used for the coupling of energy into tissue for the induction of localized hyperthermia. These include: ultrasound, radiofrequency and microwave coupling. As discussed in Chapter 1, uniform heating is generally not possible with these methods because of variable blood flow rates and inhomogeneities in the tissue. By integrating the volumetric energy absorption rate $\mathring{q}a'$, which is both tissue and source specific over the

control volume, the total energy, $\dot{q}a$, absorbed in the control volume can be found

$$\dot{q}a = \int_V \dot{q}'a \, dV \qquad \ldots(2.7)$$

A specific energy input term for the modality under consideration is usually implemented.

Considering these five mechanisms of heat transfer in a heat balance then yields

$$\frac{d}{dt}\int_V pcT \, dV = \int_A kij\frac{dT}{dxj} \, ni \, dA + \int_A cb \cdot Tb \cdot fi \cdot ni \, dA + \int_V \dot{q}'m \, dV + \int_V \dot{q}'a \, dV \qquad \ldots(2.8)$$

Which describes the in-vivo conservation of thermal energy for a tissue absorbing energy from an external source. The Bioheat equation is found by rewriting equation(2.8) in differential form, assuming volume average blood perfusion rates.(3)

$$pc\frac{dT}{dt} = \nabla(k\nabla T) + \dot{q}'m + \dot{q}'a + wb \cdot cb(Ta-T) \qquad \ldots(2.9)$$

2.3 METHODS OF SOLUTION

By identification of the pertinent electrical and thermal tissue parameters as well as existing boundary conditions the differential equation can, in principal, be solved analytically. However due to its complexity, a closed form solution is nearly impossible for all but the simplest cases. However the use of numerical methods can simplify the problem. The basic principle of the numerical approach to a heat conduction problem is the replacement of the differential equation for the continuous temperature distribution by a finite-difference or finite-element equation which must be satisfied at certain points within the medium. Numerical techniques can easily deal with irregular geometries, boundary conditions, temperature and spatially dependent properties, nonhomogeneous perfusion and nonuniform SAR distribution parameters. These parameters are at best difficult to deal with using analytical methods of solution in all but the simplest cases. Finite-difference methods are generally easier to program for simple problems and require less storage and computer time to run, but complex boundary geometries with variable properties become difficult to handle when compared to finite-element methods.

For the numerical approach, anatomical boundaries of tumor and normal tissues must be distingiushed. CT-scans are becoming popular in radiotherapy treatment planning and can

play an important role in this respect when planning a hyperthermic treatment. Tissue properties which must be known include:

1. Thermal properties such as the thermal conductivity(k), the density(p) and the specific heat(c).
2. Electrical properties such as the permittivity(ξ) and the electrical conductivity(δ), are also important.

In addition, surface boundary conditions must be defined. That is, the heat transfer coefficient at the tissue surface must be known in addition to the environmental temperature. Furthermore, the physiological response characteristics of both the normal and tumor tissues must be understood. This includes some knowledge of the perfusion field as discussed above. In the clinical setting, one of the most important questions to be answered concerns extremes of temperature.(8) That is, a low tumor temperature implies insufficient heating is occuring, while a high normal tissue temperature indicates that the normal tissue is incurring damage.

The bioheat transfer equation does not explicitly account for the presence of large blood vessels containing relatively cool blood which could reduce the temperature in the tumor tissue adjacent to the vessel.(9,10) It is however, possible to account for this by raising (wb) to large values in positions where these vessels occur. As the

modelling performed in this work concerns general situations, typical standardized values of tissue properties are used as are idealized anatomical models. In many cases clinically, the only significant unknowns include the nature of the thermal model of the tumor, highly dependent upon blood flow conditions, and the characteristics of the blood flow response of normal tissues to heat. Standardized tumor and patient models however, can be used in a systematic fashion to account for these unknowns.

In using the bioheat transfer equation, the power deposition patterns of the various heating systems are determined with respect to the volume of interest(SAR distribution), and this information is then used in a numerical model of the bioheat equation to calculate the resulting temperature distributions.

To start, the power deposition, Qp, must first be determined. This may be determined theoretically using a mathematical model of power deposition. For electromagnetic radiation

$$Qp(\vec{r},t) = \sigma(\vec{r}) \left| E(\vec{r},t) \right|^2 \qquad \ldots(2.10)$$

Where, σ = the electrical conductivity (mho/m)

E = electric field (V/m).

Most electromagnetic hyperthermia systems operate at a single frequency in the continuous wave mode. The power

levels are controlled by changing either, the amplitude of the wave or, less frequently, by pulse width modulation.

Static phantoms (simple homogeneous or layered) can be used to verify the power deposition patterns while more complicated phantoms, simulating realistic dimensions and anatomical features can be used to study the effect of heterogeneities on the SAR distribution. The SAR distribution can then be superimposed on a thermal model of the tissues and the temperature distribution calculated. Note also that the efficacy of hyperthermia resides not on the power deposition, but on the temperatures reached, which are a result of the net differences between power delivered and power removed. In the future more detailed models will require further knowledge of the variations in the arterial temperature, probably coupled with an improved version of the bioheat transfer equation which also includes flow directionality effects and the effects of large vessels.(11)

2.4 REFERENCES

1. Bentzen S.M., et al, Radiotherapy and Oncology, 2,255-260,1984

2. Strohbehn J.W., Roemer R.B., IEEE Trans. BME 31(1),136-149,1984

3. Bowman H.F., National Cancer Institute Monograph 61,437-445,1982

4. Cravalho E.G., et al, Thermal Char. of Tumors:Application in Detection and Treatment, Jain R.K., Gullino P.M.(eds).Ann. NY. Acad. Sci. 335,86-97,1980

5. Emery A.F., Therapeutic Heat and Cold:Computer Modeling of Thermotherapy Lehmann J.K.(ed), Baltimore:Williams and Wilkins,133-171,1982

6. Jain R.K., Bioheat Transfer:Mathematical Models of Thermal Systems: Hyperthermia in Cancer Therapy. Storm F.K.(ed) Boston:Hall, 9-46,1983

7. Pennes H.H., J. Applied Physiology. vol.1(2),93-122,1948

8. Roemer R.B., Cetas T.C., Cancer Research (suppl.) 44,4788s-4798s,1984

9. Lagendick J.J.W., Phys.Med.Biol.,vol.27(1),17-23,1982

10. Chato J.C., Trans. of the ASME,vol.102,110-118,1980

11. Wulf W., Thermal Char. of Tumors:Application in Detection and Treatment, Jain R.K., Gullino P.M.(eds). Ann.NY.Acad.Sci. 335,151-153,1980

Chapter III

INTRODUCTION TO FINITE DIFFERENCE TECHNIQUES

3.1 SOLVING THE BIOHEAT EQUATION

The bioheat equation, derived in Chapter 2, may be expressed in the form

$$pc \frac{dT}{dt} = \nabla(k \nabla T) + \acute{qm} + \acute{qa} + wb \cdot cb(Ta-T) \quad ...(3.1)$$

which must be solved in some spatial region within a boundary.

Solutions must be found which satisfy certain constraints, called boundary conditions which are an inherent part of even the general solution to the problem. Depending on the numerical procedure used, explicit or implicit, it may or may not be necessary to solve a system of linear algebraic equations. With explicit methods the solution proceeds by simple replacement with the size of the time step limited by stability considerations. These constraints can be partially or totally removed by the use of implicit methods, at the expense of then having to solve systems of equations. A third approach can also be used, which calculates alternate temperatures in a grid, both implicitly and explicitly, thus combining the speed and

simplicity of explicit methods with the accuracy and stability found in implicit methods. This latter method will be discussed in Chapter 4.

The finite difference approximations to the first and second derivatives of a given function are presented in this chapter. These finite difference equations are then applied in the solution of the one-dimensional bioheat equation given in equation(3.2) below.

3.2 NUMERICAL SOLUTION OF THE BIOHEAT EQUATION

3.2.1 Derivation of the Finite Difference Equations

The 1-D bioheat equation is given by the expression

$$pc \frac{dT}{dt} = k \frac{d^2T}{dx^2} + [\, H(x)-C(x,T) \,] \qquad ...(3.2)$$

Where the metabolic term $\dot{q}m$ has been neglected and H(x) and C(x,T) represent the power input and cooling terms respectively.

To derive the finite difference equations first consider the function f(x) shown in Figure(3.1). The points x1,xo,x2 are equally spaced with xo-x1 = x2-xo = Δx on a 1-D grid. That is, xi = xo +i Δx and the values are denoted by the function f(x) where $fi = f(x)\Big|_{x=xi}$. An estimate of the derivative of f(x) at x=xo- $\Delta x/2$ is

$$\left.\frac{df}{dx}\right|_{x=xo-\Delta x/2} = \frac{fo-f1}{\Delta x} \qquad ...(3.3)$$

Based only on f1 and fo.

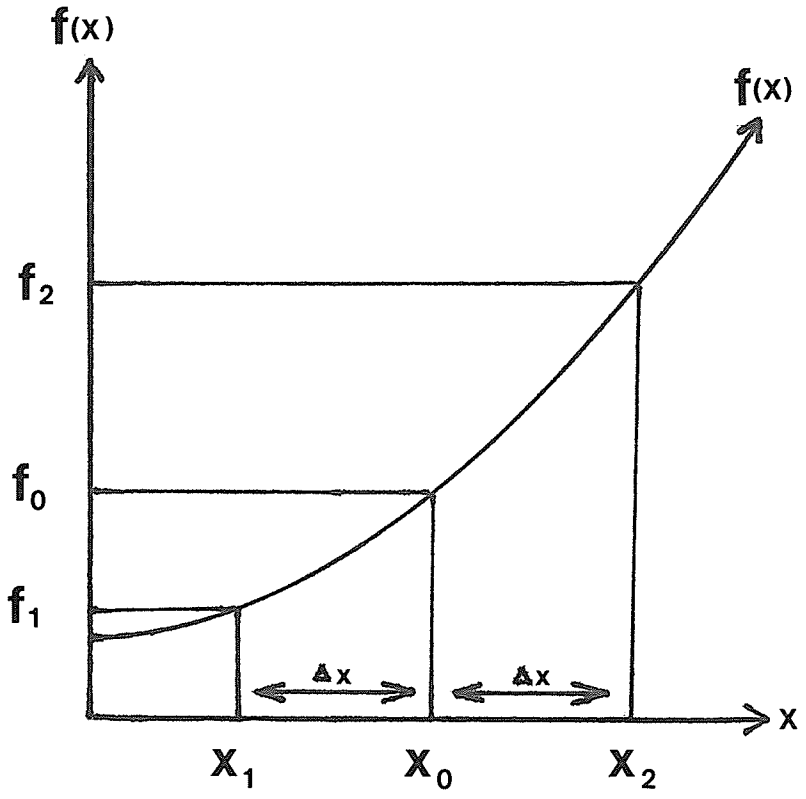

Figure 3.1

Curve showing the values f_1, f_0, f_2 of the function f(x) taken at equally spaced points x_1, x_0, x_2 seperated by distance Δx between successive points.

The derivative of f(x) at $x=xo+\Delta x/2$ is estimated by

$$\left.\frac{df}{dx}\right|_{x=xo+\Delta x/2} = \frac{f2-fo}{\Delta x} \qquad ...(3.4)$$

Based only on fo and f2.

Both (3.3) and (3.4) are an approximation to df/dx at x=xo and they are thus referred to as 1-sided differences. A more accurate estimate however, could be made by using the two points on either side of xo:

$$\left.\frac{df}{dx}\right|_{x=xo} = \frac{f2-f1}{2\Delta x} \qquad ...(3.5)$$

This is called a central difference estimate based on the two values of f1 and f2.

The second derivative of f(x) at x=xo may be found by estimating the first derivative in each of the two intervals (x1,xo) and (xo,x2) and dividing their difference by the distance between the two points.

Thus

$$\left.\frac{d^2f}{dx^2}\right|_{x=xo} = \left.\frac{d}{dx}\left(\frac{df}{dx}\right)\right|_{x=xo}$$

$$= \frac{\left.\frac{df}{dx}\right|_{x=xo+\Delta x/2} - \left.\frac{df}{dx}\right|_{x=xo-\Delta x/2}}{\Delta x}$$

$$= \frac{\frac{(f2-fo)}{\Delta x} - \frac{(fo-f1)}{\Delta x}}{\Delta x}$$

$$= \frac{f1-2fo+f2}{(\Delta x)^2} \qquad ...(3.6)$$

From the above derivation it can be seen that the accuracy improves as Δx becomes smaller.

Using equation(3.6), the x-derivative in equation (3.2) may be written as,

$$(\Delta x)^2 \frac{d^2T}{dx^2} = [\, T(x-\Delta x,t) - 2T(x,t) + T(x+\Delta x,t) \,] \qquad ...(3.7)$$

For the time derivative in equation (3.2) we may write, from (3.3),

$$\frac{dT}{dt} = \frac{T'(x) - T(x)}{\Delta t} \qquad ...(3.8)$$

where, $T'(x)$ is the temperature at the next time increment. Upon substituting (3.7) and (3.8) into equation (3.2) we have

$$pc\,\frac{(T'(x)-T(x))}{\Delta t} = k\,\frac{[\, T(x-\Delta x,t) - 2T(x,t) + T(x+\Delta x,t) \,]}{(\Delta x)^2} + [\, H(x,y)-C(x,T) \,] \qquad ...(3.9)$$

Thus, equation(3.9) is the finite difference representation of equation (3.2). It may be solved to yield the 1-D time dependent temperature.

3.2.2 The Grid System

In using finite difference techniques to solve partial differential equations a network of grid points must be

established throughout the region of interest. The points are taken to be the point of intersection of a grid covering a continuous region in 2-D. In this manner a discrete approximation of a continuous 2-D region may be obtained.

In the case of the transient problem a third coordinate time (t) is taken outwards from the page and the 2-D grid is repeated at intervals of Δt outwards making a 3-D grid system. Thus instead of developing a solution which is valid everywhere in the region only approximations are made at discrete points. By making the grid system sufficiently small it is expected that the approximate solution will be sufficiently accurate.

3.2.3 Environmental Boundary Conditions

Boundary condition specification constitutes a major input to the heat transfer problem. The parameters which must be considered include:

1. Interactions: Usually the heat conduction problem cannot be separated from the associated problem of characterizing radiative surface cooling conditions.
2. Transients: The general heat conduction problem is time-dependent, but if the conductivity(s) is(are) time independent, the temperature distribution becomes steady after prolonged exposure. The exposure time for this is short if the conductivity

is large and vice versa. This represents the special case of steady-state heat conduction, the solution of which may be achieved by time-tracking the associated time- dependent problem. Conditions of steady-state temperature and heat conduction are always preceded by a starting transient t of finite duration.

3. Initial and Final States: The exposure problem occurs when a body is suddenly exposed at time t=0 to another environment of different temperature, and heat transfer at the surface operates to try to alter the body temperature. The body then gains or loses heat and its surface temperature tends to approach that of its surroundings, the rapidity of this change being dependent on the surface heat transfer coefficient h. The instantaneous temperature at the surface depends on the relative magnitude of h/k. If this ratio is relatively large the surface temperature tends to approach the ambient temperature quite rapidly.

3.2.4 Boundary Problems in Finite Difference Techniques

In heat transfer problems two cases often arise for boundary points:

1. The boundary surface temperature is known (Dirichet boundary condition) in which case Tb=Tg where Tg is the known temperature given in the problem

specification. Without this, Tb would occur in a set of unknowns and the problem would not be closed.

2. The boundary surface temperature is not known (Neumann derivative boundary condition) in which case the additional problem specification is in the form of knowledge about the outward normal gradient of temperature dT/dn, where n is the unit normal vector. This may be defined as

$$dT/dn = -h(Tb-Ta)/k \qquad \ldots(3.10)$$

where, h is the surface heat transfer coefficient(which is usually taken to be known beforehand but is actually dependent on the circumstances in question), k is the thermal conductivity and Tb and Ta are the boundary and ambient temperatures respectively.

Consider the simple case shown in Figure(3.2). The finite difference equations can be derived using the direct partial differential equation replacement; equation (3.4) above. This method requires the introduction of a fictitious node point(f) at a distance Δx from the surface node b. It cannot be assumed that Tf=Ta however since Tf is affected by the presence of the body whereas Ta is the ambient temperature far from the body.

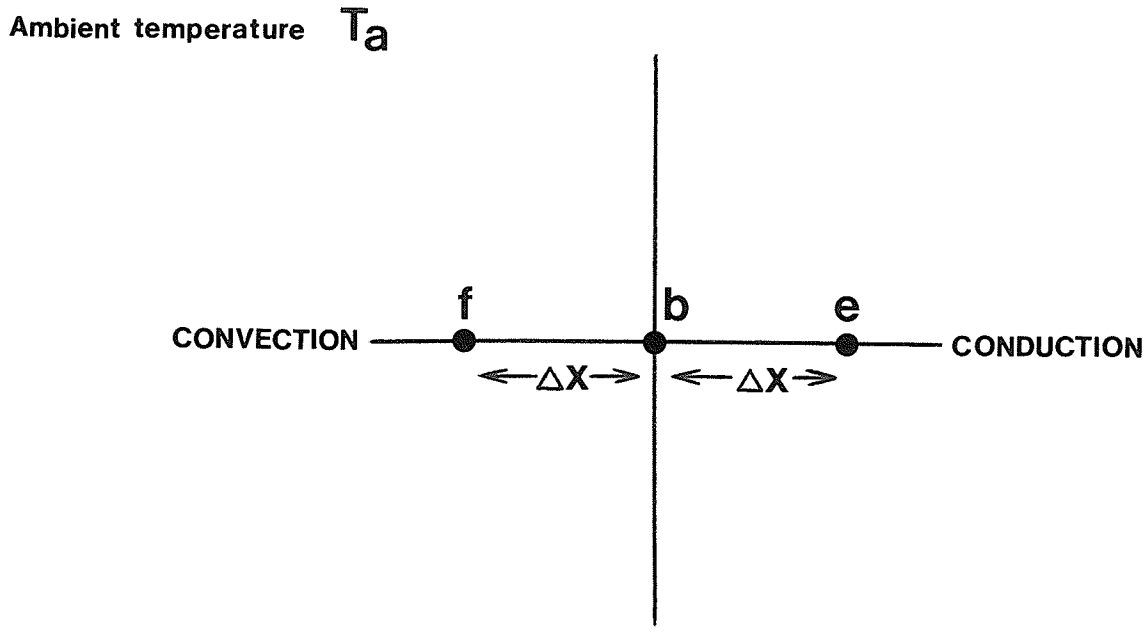

Figure 3.2

Introduction of a fictitious nodal point (f) near a convective boundary surface of a 2-D body. A square mesh is used.

The usual finite difference equation for point b is therefore applied introducing the temperature at the fictitious point f. This is then eliminated by a central difference approximation to dT/dn at b. Thus

$$\frac{Tf-Te}{2\Delta x} = \frac{-h}{k}(Tb-Ta) \qquad \ldots(3.11)$$

Equation (3.11) is then solved for Tf and substituted into the given finite difference equation thereby eliminating the unknown fictitious temperature Tf.

3.3 THE FINITE DIFFERENCE EQUATION

The 1-D finite difference equation can be written as

$$T'(x) = \frac{k\,\Delta t}{pc\,(\Delta x)^2}[T(x1)-2T(x)+T(x2)] + T(x) + \frac{\Delta t}{pc}[A\exp(-x/L)-V(T(x)-To)] \qquad \ldots(3.12)$$

where, x is the spatial parameter representing depth with x=0 on the surface.

$x1 = x - \Delta x$

$x2 = x + \Delta x$

L is the depth of penetration

$A\exp(-x/L)$ is the power input term

Let, $Q = \frac{k\,\Delta t}{pc\,(\Delta x)^2}$ and $R = \frac{\Delta t}{pc}$

Then,

$$T'(x) = Q\,[T(x1)-2T(x)+T(x2)] + T(x) + R\,[A\exp(-x/L)-V(T(x)-To)] \quad ...(3.13)$$

In finite difference form the surface cooling condition is expressed from (3.11) above by

$$\frac{T(x1) - T(x2)}{2\Delta x} = \frac{-h\,(T(x)-TA)}{k} \quad ...(3.14)$$

Solving for T(x1) we have

$$T(x1) = \frac{-2\Delta x h}{k}\,(T(x)-TA) + T(x2) \quad ...(3.15)$$

at the surface where x=0. Therefore in summary, when x=0 we have

$$T'(x) = Q\,[2\Delta x \propto (TA-T(x))+2(T(x2)-T(x))] + T(x) + R\,[A\exp(-x/L)-V(T(x)-To)] \quad ...(3.16)$$

where, $\propto = h/k$ and when $x > 0$ we have

$$T'(x) = Q\,[T(x1)-2T(x)+T(x2)] + T(x) + R\,[A\exp(-x/L)-V(T(x)-To)] \quad ...(3.17)$$

3.4 STABILITY AND CONVERGENCE CONSIDERATIONS

Two types of errors may occur

1. Truncation error:Due to computing with derivatives replaced by finite differences. Depends on the initial given temperature distribution, boundary conditions, choice of finite difference scheme and choice of Fourier number (Fo) used in computation. The Fourier number is a dimensionless group used to

define the stability of transient heat flow calculations: The Biot number is also used to this same effect.

$$Fo = \frac{k\ \Delta t}{p\ c(\Delta x)^2} = \frac{\text{rate of conduction of heat}}{\text{rate of storage of heat}} \quad \ldots(3.18)$$

The Fourier number gives an indication of the speed at which a body will respond to a temperature change. A low value of Fo implies that a long period of time is required to heat or cool the body. The Biot number is defined as

$$Bi = \frac{h\,\Delta x}{k} = \frac{\text{surface conductance}}{\text{internal conductance}} \quad \ldots(3.19)$$

Table(3.1) summarizes the conditions which must be met for various grid points(2). Thus Δt is chosen, for a given grid system, so that the coefficient of T(x) is non-negative. Following this rule, stability will not be affected by the addition of a constant internal heat generation term.

2. Numerical errors:These are round-off errors caused by the finite significant figure restriction used in any calculation. The floating point system on the computer used carried nine significant figures and therefore round-off errors were not a concern in this work.

In general if the solution is unstable, the computed values will oscillate with increasing magnitude as the calculation proceeds. The space and time increments Δx and Δt

Table 3.1

Interior nodes:

1-D cartesian	$F_o \leqslant 1/2$
2-D cartesian	$F_o \leqslant 1/4$
3-D cartesian	$F_o \leqslant 1/6$
Hexagonal	$F_o \leqslant 3/4$

Boundary nodes(convective):

1-D cartesian	$F_o \leqslant 1/(2(1+Bi))$
2-D cartesian	$F_o \leqslant 1/(2(2+Bi))$
2-D cartesian(corner node)	$F_o \leqslant 1/(4(1+Bi))$
3-D cartesian	$F_o \leqslant 1/(2(3+Bi))$

therefore cannot be selected arbitrarily but must satisfy the stability criteria established above. Thus Δt should be chosen, for a given spatial subdivision, so that the coefficient of T is non-negative. This is a sufficient condition for the stability of explicit finite difference equations.

3.5 VERIFICATION BY COMPARISON WITH AN ANALYTICAL SOLUTION

Equations (3.16) and (3.17) were compared to a 1-D analytical solution given by Foster(3) of the form

$$T(x) = \frac{A/k}{bf-1/L^2}\left| e^{(-x/L)} - \frac{1/L+\alpha}{\alpha+\sqrt{bf}} e^{(-x\sqrt{bf})}\right| + \frac{\alpha(TA-To)}{\alpha+\sqrt{bf}} e^{(-x\sqrt{bf})} + 37 \quad \ldots(3.20)$$

where, TA is the ambient temperature

To is the body core temperature

The energy input for a plane electromagnetic wave of intensity Io in W/cm2 incident upon the tissue is given by:

$$Q = \frac{Io\tau}{JkL} \exp(-x/L) = A \exp(-x/L) \quad \ldots(3.21)$$

where, $A=Io\tau/JkL$

J:the mechanical equivalent of heat

L:depth at which microwave power is reduced by e.

τ:the fraction of energy transmitted into the tissue

k:the tissue conductivity

The analytical and finite-difference solutions matched to within 0.01 ^{o}C at all depths for a wide range of surface cooling, heat input and blood flow conditions.

3.6 REFERENCES

1. Chan A.K.,IEEE Trans.Bio.Med.Eng.20(2),86-90,1973

2. Croft D.R.,Lilley D.G.,Heat Transfer Calculations Using Finite Difference Equations:Applied Science Publishers Ltd.,1977

3. Foster K.R., Kritikos H.N., Schwan H.P., IEEE Trans. Bio. Med. Eng. 25(3),313-316,1978

Chapter IV

PERTURBATIONS IN THE STEADY-STATE TEMPERATURE DISTRIBUTION CAUSED BY THE PRESENCE OF METALLIC THERMOMETERS

4.1 SELF-HEATING OF METALLIC THERMOMETERS

4.1.1 Introduction

As stated in Chapter 1, one of the more significant problems in regional and local hyperthermia treatments is that of determining the temperature distribution in and around the target volume. For the purposes of planning, application and assessment of any hyperthermia treatment, a knowledge of the temperature distribution is essential. To date such distributions cannot be measured directly but must be calculated from measurements taken invasively at a few selected locations. The accuracy with which such temperature information is required may be deduced from biological studies(Chapter 1). It has been shown, that for a given level of damage to either cells in vitro or tissues in situ, at therapeutic temperatures above 42 ^{o}C, a change of 1 ^{o}C is equivalent to a change in heating time by a factor of two.(1)

Significant temperature measurement problems however may be encountered when electromagnetic energy is employed in a

hyperthermia treatment if thermometers, which couple to the electromagnetic field, are positioned in the field while the power is on. The effects include: artefacts in the sensitive amplifiers employed with such thermometry systems; perturbations in the SAR distribution as a result of re-radiation of the incident EM-energy from the wires; and the direct heating of the metallic thermometers under microwave irradiation. Artifactual temperature measurements can occur as a result of this self-heating of the thermometer wires. A quantitative analysis of this latter effect was the subject of a previous study.(2)

This Chapter focuses on the effect of the heat produced in the thermometer wires on the steady-state temperature distribution. A quantitative study, of the effects of thermometer size, position and coupling efficiency as well as an assessment of the effects of blood flow on the temperature perturbations produced in the neighborhood of the thermometer is presented below. Input data covering a wide range of parameters which could be encountered in the clinical setting were used. The results permit a realistic assessment of the consequences for microwave hyperthermic dosimetry involving the use of metallic thermometers.

4.2 THEORY

Metallic wires placed in an EM-Field can act to alter the steady-state temperature distribution in the surrounding tissue as a result of their self-heating. It is well known that this effect can be minimized by orienting the wires perpendicular to the incident electric field if such a direction is defined.(3) However, even with irradiation by a plane polarized wave, it may not be possible to eliminate this problem as reflections at tissue boundaries can alter the direction of polarization. Thus it can be assumed that some component of the E-field will fall along the wires and consequently the conversion of microwave energy into heat will occur.

For a thermocouple/catheter assembly(Figure(4.1)) the degree of self-heating may be described by the Enhancement Factor (EF) of the probe. The enhancement factor is defined as the ratio of the heat generated per unit length of the assembly to that produced by the same local microwave field in the same volume of tissue. Thus the enhancement factor is a function of the coupling efficiency of the incident EM wave with the metallic wires of the probe and its encapsulating material and represents the additional amount of incident microwave energy that is converted into heat by the assembly when compared to an equivalent volume of tissue. Dunscombe(3), reported that the heat generated per

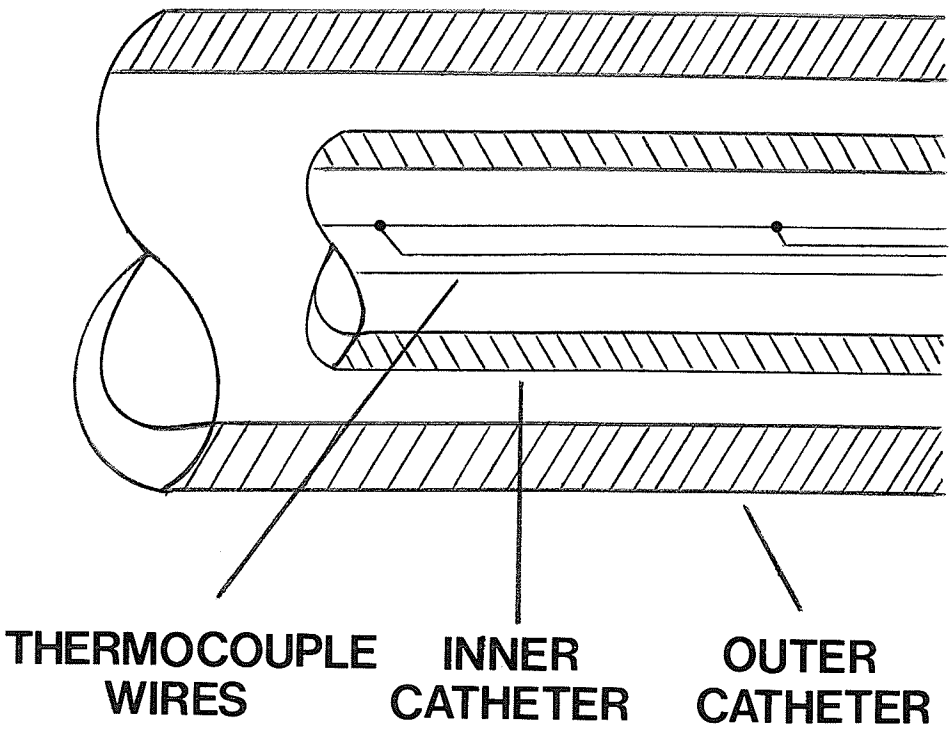

Figure 4.1

Schematic representation of the design of an array assembly.

unit length in a thermocouple array assembly of outside diameter 1.7mm and under circularly polarized 2450 MHz irradiation was as much as six times that which would be generated in the same volume of muscle like tissue. The values of the enhancement factors chosen for the current studies therefore cover a range about this figure.

Since the main concern here is with the temperature perturbation produced in the tissue surrounding the array assembly and not in the temperatures achieved within the assembly (assembly meaning wires and surrounding catheters) and since the calculations are performed for steady-state temperatures, the assembly may be considered solely as a heat source.

A 2-Dimensional Finite Difference program using Gourlay's Hopscotch technique (4) and an irregular grid in rectilinear coordinates was developed for use on a PDP-11 computer in order to model several different conditions which could be encountered in the clinical environment.

The temperature distribution is obtained from equation(3.2) of the form:

$$pc \frac{dT}{dt} = \nabla(k \nabla T) + H + C \qquad \ldots(4.1)$$

Where, T is the temperature distribution in ^{o}C

k thermal conductivity of muscle tissue

p density of tissue

c specific heat tissue plus blood

H heat input due to microwave field

C heat sink term representing the cooling due to blood flow

Metabolic effects have been ignored(see Chapter 2).

Using the finite difference method of Croft et al(6) and extending equation(3.12) to 2-D we can write

$$T(u,v,j+1) = \frac{k\,\Delta t}{pc}\left[\frac{T(u+1,v,j)-2*T(u,v,j)+T(u-1,v,j)}{(\Delta x)^2} + \frac{T(u,v+1,j)-2*T(u,v,j)+T(u,v-1,j)}{(\Delta y)^2}\right] + T(u,v,j) + \frac{\Delta t}{pc}[H(u,v)-C(u,v)] \quad \ldots(4.2)$$

Where, the subscripts u,v and j are the increment indices for the spatial coordinates x,y and time coordinate t respectively.

The thermal source function H(u,v) describes the rate of heat production and is related to the Specific Absorption Rate. For a plane EM wave of intensity Io (W/cm2) propagating through tissue the power loss varies with distance from the energy source as

$$H(x,y) = Q * EF * \exp(-x/L) \quad \ldots(4.3)$$

Where, L (1/depth of penetration) 0.85 cm at 2450 MHz

$Q = Io\tau/JL$

J mechanical equivalent of heat

τ fraction of energy transmitted into tissue: for

muscle tissue $\tilde{T}$=0.4 at 2450 MHz

EF=1 for muscle tissue by definition

Note:That EF=1 everywhere except where the wire is positioned. This region (where EF≠1) is so small that L is assumed unchanged by the presence of the thermometer assembly.

The cooling function is a heat sink term of the form

$$C(x,y,T)= V*(T-To) \qquad ...(4.4)$$

Where, V is the product of blood flow and the specific heat of blood.

To is the core temperature 37 ^{o}C and represents the temperature of the blood entering the tissue.

The surface boundary condition is of the Neumann type(6) as described by equation(3.15) in Chapter 3.

4.3 CARTESIAN COORDINATES: IRREGULAR GRID

An irregular grid was used to save time and memory space. The derivation of the required finite difference equation is shown below. The calculations are similar to those presented in Chapter 3 using a regular grid, with the values now weighted according to their position relative to the grid.

4.3.1 Functional Derivatives in an Irregular Grid

Consider the typical function shown in Figure (4.2). For unequally spaced points x1,xo,x2 on a 1-D grid, the following case may be defined where $x2-xo = a\Delta x$, $xo-x1 = b\Delta x$ for all $(0 \leqslant a, b \leqslant 1)$. Both forward and backward difference estimates of the derivative of f(x) at x=xo can be made. The forward difference is estimated at $xo+.5a\,\Delta x$, the midpoint between xo and x2, in terms of f2 and fo as

$$\frac{df}{dx} = \frac{f2-fo}{a\,\Delta x} \qquad \ldots(4.5)$$

and the backward difference at $xo-.5b\,\Delta x$, the midpoint between x1 and xo, in terms of f1 and fo as

$$\frac{df}{dx} = \frac{fo-f1}{b\,\Delta x} \qquad \ldots(4.6)$$

A central difference estimate can then be made by taking a weighted average of the two one sided derivatives: weighted in favour of the nearer estimate as

$$\left.\frac{df}{dx}\right|_{x=xo} = \frac{a}{a+b}\left(\frac{df}{dx}\right)_{xo-.5b\Delta x} + \frac{b}{a+b}\left(\frac{df}{dx}\right)_{xo+.5a\Delta x}$$

$$= \frac{1}{(\Delta x)}\left[\frac{b\ f2}{a(a+b)} - \frac{(b-a)\,fo}{ab} - \frac{a\ f1}{b(a+b)}\right] \qquad \ldots(4.7)$$

Similarly, to estimate the second derivative of f(x) at x=xo, the difference in the two one-sided derivatives, estimated at the midpoints of x1 to xo and xo to x1 respectively, is divided by the distance between them, $.5(a+b)\,\Delta x$. This actually estimates f"(x) at $x=xo+.5(a+b)$

Δx . But this value is retained as it is the best estimate for the value at xo based on the 3-function values.

Thus

$$\frac{d^2f}{dx^2} = \frac{\left| \left.\frac{df}{dx}\right|_{x=xo+.5a\,\Delta x} - \left.\frac{df}{dx}\right|_{x=xo-.5b\,\Delta x} \right|}{\left| \frac{(a+b)\,\Delta x}{2} \right|}$$

$$= \frac{2}{(\Delta x)^2}\left| \frac{1}{a(a+b)}\,f2 - \frac{1}{ab}\,fo + \frac{1}{b(a+b)}\,f1 \right| \qquad ...(4.8)$$

A similar argument holds for the y-direction.

The 2-D finite difference form for the steady state equation with a nonuniform grid may then be represented as

$$\frac{2}{(\Delta x)^2}\left| \frac{1}{a(a+b)}T(x1,y) - \frac{1}{ab}T(x,y) + \frac{1}{b(a+b)}T(x2,y) \right|$$

$$+ \frac{2}{(\Delta y)^2}\left| \frac{1}{c(c+d)}T(x,y1) - \frac{1}{cd}T(x,y) + \frac{1}{d(c+d)}T(x,y2) \right|$$

$$\frac{H}{k} + \frac{C}{k} = 0 \qquad ...(4.9)$$

where, H and C are evaluated at (x,y) if they vary with position or temperature, and c and d have been defined in the y-direction as

$$y2-yo = c\,\Delta y$$

$$yo-y1 = d\,\Delta y$$

Notice that setting a,b,c,d equal to unity retrieves the uniform grid form of equation(4.2) above. The transient case, with the blood flow term included, may be written as

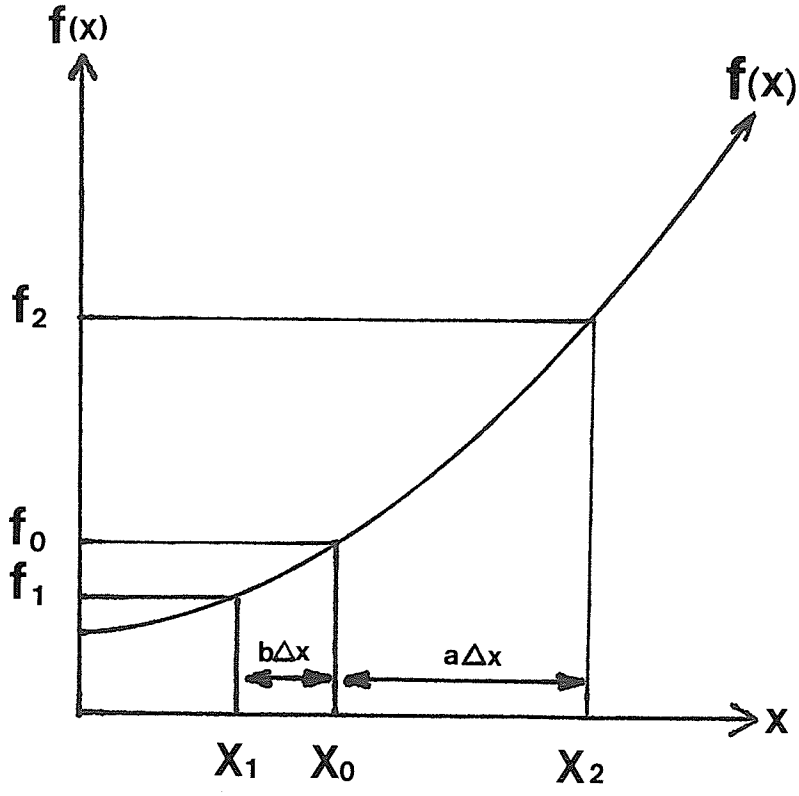

Figure 4.2

Curve showing the values f_1, f_0, f_2 of the function f(x) taken at unequally spaced points x_1, x_0, x_2 where,

$$x_2 - x_0 = a\Delta x$$
$$x_0 - x_1 = b\Delta x \quad (0 \leq a, b \leq 1).$$

$$\text{L.H.S.of eq(4.9)} - \frac{C(x,y,T)}{k} = \frac{pc}{k}\left|\frac{T'(x,y) - T(x,y)}{\Delta t}\right| \qquad \ldots(4.10)$$

with the notation $T'(x,y)=T(x,y,t+\Delta t)$ and all other non-primed quantities are evaluated at time t. Equation(4.10) was implemented for the calculations performed in this chapter using the heat input and heat sink terms of the form given in equations (4.3) and (4.4) respectively.

Gourlay's Hopscotch algorithm, derived in Appendix A, was then applied for stability and convergence considerations as well as time benefits.

The standard conditions used for the calculations were chosen to model a typical clinical situation and are listed below.(7)

$k = 0.4187\ W/m\ ^{o}C$ thermal conductivity of tissue

$pc = 4.187E6\ J/m^{3}\,^{o}C$

$Q = 1.67E5\ W/m^{3}$ for a blood flow of 5ml/100g/min

$V = 3.48E3\ W/m^{3}\,^{o}C$

$h = 4.187E3\ W/m^{3}\,^{o}C$

$\alpha = h/k = 100/m^{2}$

The standard cross section of the assembly simulated was 1mm square (which is typical of the size of invasive thermometers used clinically) and this was placed 20mm below

the surface of the homogeneous tissue. The value of EF unless otherwise stated was 10.

Before the trials were performed the 2-D finite difference technique, with a power input uniform in the y-direction (plane wave irradiation) was compared with the 1-D analytical solution given in Chapter 3. The curves matched to within 0.01 ^{o}C from the surface (x=0) to a depth of 5 cm.

A typical temperature profile, with a perturbation in the temperature distribution from an assembly placed at 20mm depth using an exaggerated enhancement factor (EF=30) is shown in Figure(4.3). The parameter used to quantify the thermal perturbation was ΔT where $\Delta T = T - T1$, T is the temperature in the tissue immediately next to the thermocouple and T1 is the temperature in the same location without the thermocouple in place. Therefore ΔT is a measure of the amount by which the temperature distribution is perturbed by the presence of a thermocouple assembly. Note, in the discrete grid system used, the point immediately next to the assembly was located 0.25mm from the assembly's outer edge. The temperature gradient in this area is approximately 0.2 ^{o}C/mm.

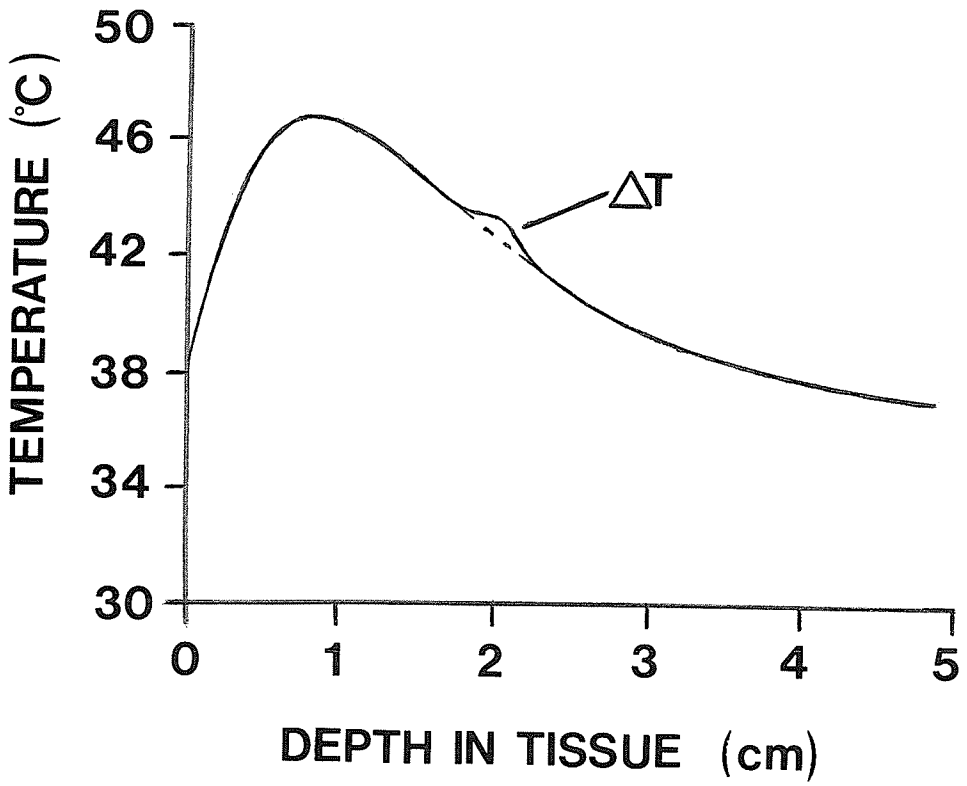

Figure 4.3

The temperature distribution in homogeneous tissue containing a perturbing thermometer (EF=30) when irradiated with plane 2450 MHz microwave radiation.

4.4 RESULTS AND DISCUSSION

The effect of the enhancement factor on the thermal perturbation is shown in Figure(4.4). It can be seen that there is a linear increase in the magnitude of the thermal perturbation with increasing EF values over the range tested.

The effect of blood flow on the magnitude of the perturbation was tested using a range of blood flow values (0 to 60 ml/100g/min.). Figure(4.5) shows the perturbation increases linearily with the blood flow rate. The variation in ΔT with blood flow is an important effect. With no blood flow the magnitude of the thermal perturbation is determined solely by the thermal conductivity of the tissue. At zero blood flow, heat is conducted out of the thermometer assembly and into the surrounding tissue thus producing a perturbation in the temperature profile. As flow rates increase the effect of blood flow on the tissue temperature dominates. That is, the tissue temperature is reduced by the increasing blood flow rates while the temperature of the assembly is not. Thus an increase in the blood flow accentuates the temperature difference between the two. This effect is qualitatively the same as the increasing temperature nonuniformity with increasing blood flow reported for interstitial hyperthermia.(8)

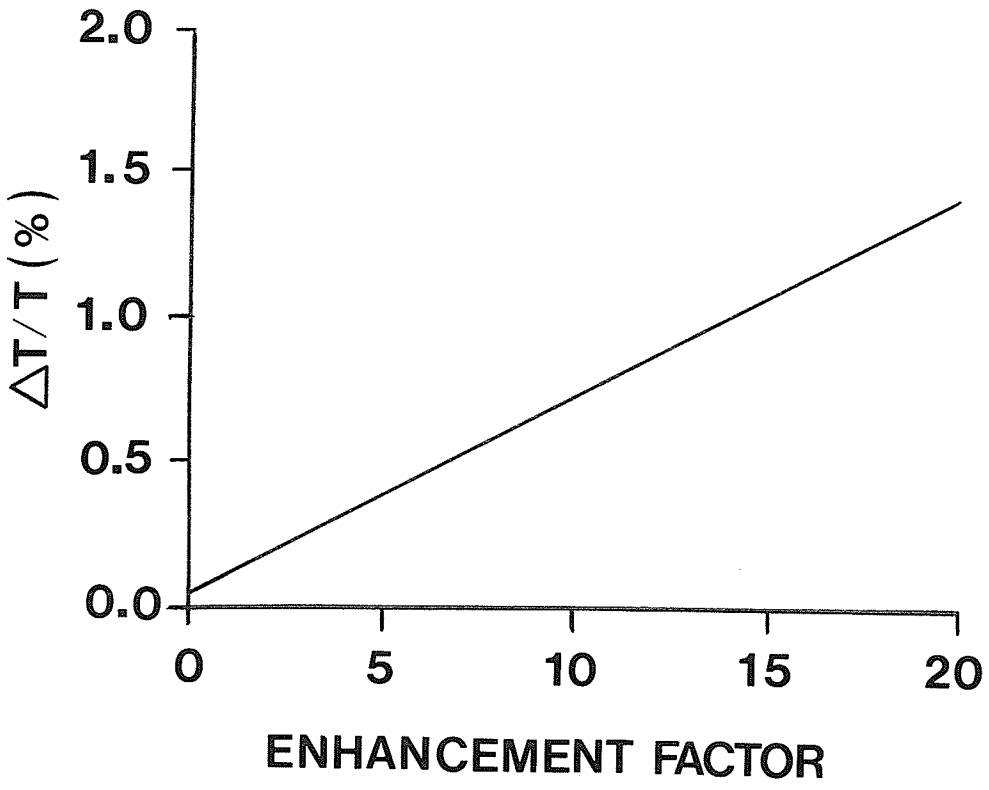

Figure 4.4

The dependence of the temperature perturbation on the enhancement factor.

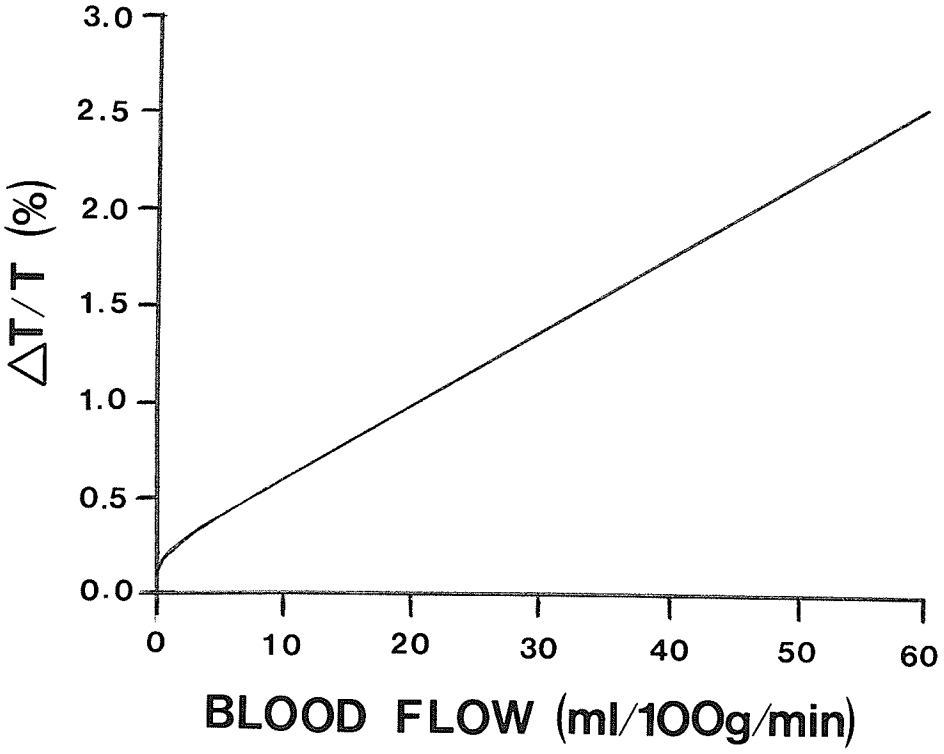

Figure 4.5

The dependence of the temperature perturbation on blood flow.

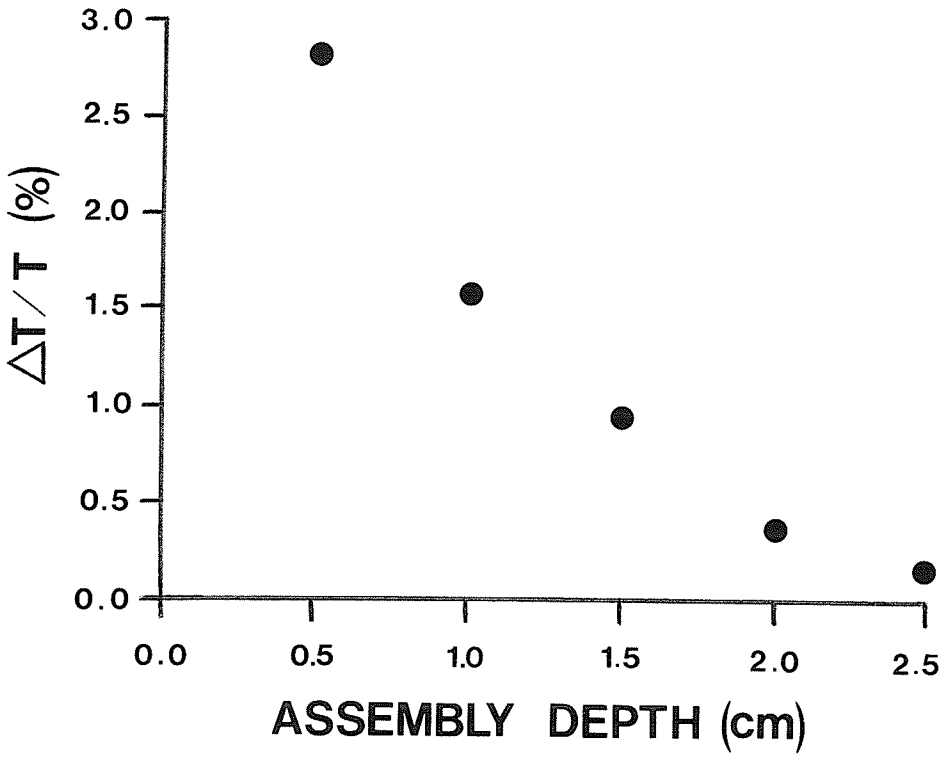

Figure 4.6

The dependence of the temperature perturbation on the depth of the assembly in tissue.

The perturbation was also measured as a function of the depth of of the assembly in tissue. Figure(4.6) illustrates that the magnitude of ΔT decreases with depth. This can be explained by noting that the ratio of the amount of heat produced with and without the assembly in place is the same at all depths and dependent only on the enhancement factor. Thus as the power density in the tissue is increased toward the surface, with a consequent increase in the heat produced, the difference between the probe temperature and that of the surrounding tissue will become more exaggerated. Hence the increase in the magnitude of the perturbation as the assembly is moved from deep within the tissue toward the surface. For depths of 10mm or more changes in the surface heat transfer coefficient (h) had little effect on the magnitude of the perturbations found. That is, $\Delta T/T\%$ changed by less than 0.1% for values of $\propto$ ranging from 0 to $500/m^2$. The data indicate that when using a perturbing thermometer in an EM-field the systematic error will increase with increasing temperature.

Outer edge sizes for the assemblies tested were increased in 0.5mm increments from 0.5mm to 3.5mm to assess the effect of total probe diameter. For each case the center of the assembly was located at 2 cm depth. A valid analysis of the effect of assembly size on the perturbation, with the other variables held constant, requires that the EF be reduced in proportion to the cross-sectional area of the assembly.

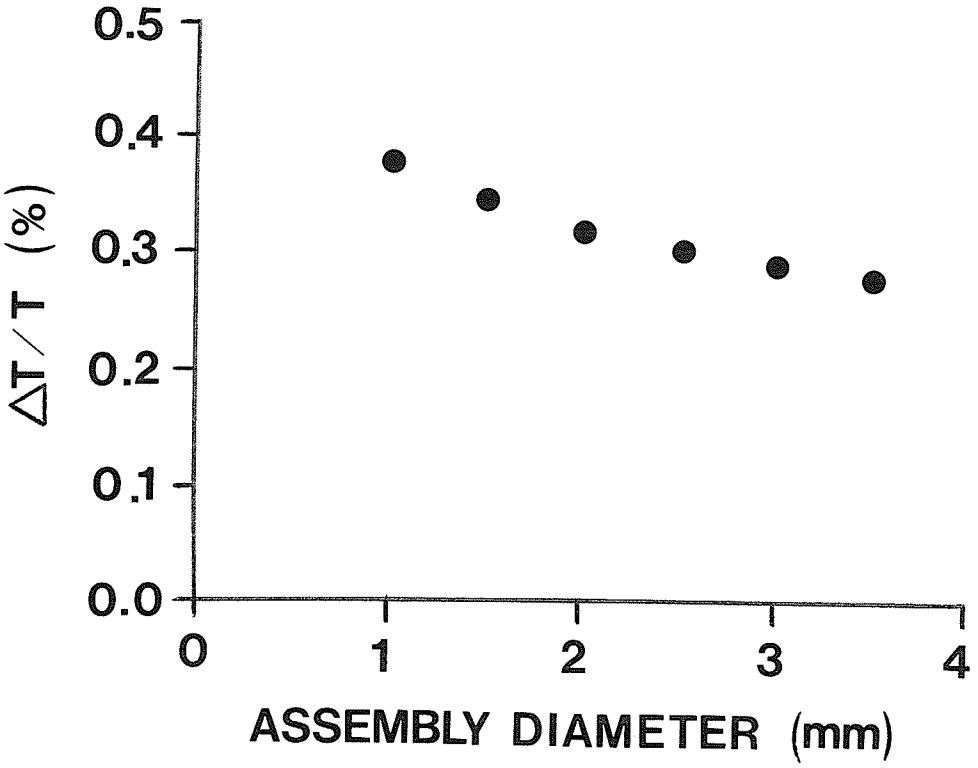

Figure 4.7

The dependence of the temperature perturbation on the size of the assembly.

Figure(4.7) shows that the perturbation decreases with increasing size of the assembly for unchanged coupling between the field and the metallic wires of the probe. With this unchanged coupling the same amount of heat is produced in the assembly independent of size. Thus as the assembly size is increased the same amount of heat is distributed across a larger area and hence its net effect is reduced. Since the difference in the size of the perturbation between a large and small probe is less than 0.2% a smaller probe would likely be of greater advantage in terms of minimizing the amount of tissue disruption during insertion.

The distance in which the perturbation extends radially outward from the assembly is small relative to the size of the tissue volume commonly heated. High blood flow rates (> 15 ml/100g/min)combined with large EF (20) values can produce a perturbation in the temperature field of at least 0.1 ^{o}C up to 2.0cm away from the assembly. Under the standard conditions however a perturbation in the temperature distribution of more than 0.1 ^{o}C is not found beyond distances of 2 to 3mm from the probe.

Under the worst conditions investigated here (i.e./EF=20,Blood flow=30 ml/100g/min ,cross-section of probe=0.5mm, placed 5.0mm below the surface), the change in tissue temperature surrounding the assembly was greater than 3 degrees celsius.

A commonly employed technique when using metallic thermometers in microwave fields is to take temperature measurements with the power off.(9) However this technique will be inaccurate if the decay rate of the temperature perturbation and that of the tissue are not identical. As will be shown in Chapter 5, the presence of changing temperature gradients and thus thermal conduction effects can influence the rate of decay of the tissue temperature. The magnitude of the errors will depend upon both the local thermal gradients and the blood perfusion levels. However, from the results presented here, it is apparent that even if an accurate extrapolation were possible, the estimated tissue temperature would still be the originally perturbed temperature and hence the residual systematic error would still not be eliminated.

4.5 CONCLUSIONS

While the increase in tissue temperature in the vicinity of the probe will have little direct effect on the tumor response due to the limited extent of the temperature perturbation, serious problems may arise due to the overestimation of the tumor temperature. Perturbations in the temperature distributions may be greater than 3 ^{o}C under conditions of elevated blood flow coupled with a high enhancement factor if the assembly is placed in the first few millimeters of tissue. These errors are of the same

order of magnitude and additive to, those errors produced by direct heating of the thermocouple wires in the region of the junction.(2) In the therapeutic temperature range, significant changes in tumor response occur with only slight changes in temperature. Consequently, clinical trials designed to evaluate the efficacy of a particular treatment regimen will be of limited value if the dosimetry is incorrect due to artifactual temperature measurements, thus emphasizing the importance of these effects.

4.6 REFERENCES

1. Field S.B., Morris C.C., Radiotherapy and Oncology,1,179-186,1983

2. Dunscombe P.B., McLellan J., Malaker K., Medical Physics,to be published.

3. Cetas T.C., Physical Aspects of Hyperthermia:AAPM Med.Phys.Monograph 8, Nussbaum G.H.(ed),New York,249-250,1982

4. Gourlay A.R., J.Inst.Maths Applics 6,375-390,1970

5. Pennes H.H.,J.Applied Physiology.vol.1(2),93-122,1948

6. Croft D.R., Lilley D.G., Heat transfer calculations using finite difference equations.Applied Science Publishers Ltd.,1977

7. Foster K.R., Kritikos H.N., Schwan H.P., IEEE Trans.BME-25(3),313-316,1978

8. Strohbehn J.W., Trembly B.S., Douple E.B., IEEE Trans Biomed.Eng. BME-29(9),649-661,1982

9. Loshek D.D., Natl. Cancer Inst. Monogr. No.61,517-519,1982

Chapter V

DETERMINATION OF BLOOD PERFUSION LEVELS USING THERMAL CLEARANCE

5.1 INTRODUCTION

Regional blood flow is an important parameter in determining the effectiveness of hyperthermia treatment in cancer therapy. As stated in Chapter 1, increases in the therapeutic ratio might be achieved by taking advantage of any differences between normal tissue and tumor tissue microvasculature. It has been proposed that because of differential tumor and normal tissue perfusion rates, a differential rise in temperature occurs between these tissues.(1) In addition, responses of tumor and normal tissue to hyperthermic challenge may be such that further damage to tumor microvasculature renders the tumor more susceptible to hyperthermia damage.(1) Thus an important task in hyperthermia is the estimation of blood perfusion rates.

Difficulties in determining perfusion levels are encountered for two reasons:

1. complex anatomical structure of the tissue and interwoven blood supply network of vessels of various sizes.

2. lack of noninvasive techniques which are capable of directly measuring such quantities.

As a result, indirect methods must be used where the required information is inferred from measurements performed on related physical and physiological parameters. Flow studies involving smaller vessels are rather complicated and less amenable to direct measurement and the results are usually presented as volume averaged blood perfusion rates. That is, nondirectional rates of blood flow through the capillary bed.(Chapter 2) The methods used include(2):

1. measurement of injected radioactive or other diffusible gasses.
2. measurement of locally generated hydrogen ions.
3. measurement of radio-labeled microspheres or aggregated albumin introduced locally into the circulation and eventually trapped in the tissue bed.
4. dissipation of heat in the tissue. That is, thermal dilution or heat clearance.

The heat clearance method is the most commonly used in hyperthermia.

Two topics will be covered in this chapter. First, the underlying physics of the thermal clearance technique is investigated. The finite difference method described in Chapter 4, with a regular grid spacing, is used to evaluate the effects of thermal conduction, power input, temperature

achieved, temperature gradients and the influence of surface cooling on the determination of the level of perfusion using the thermal clearance method.

In addition the effects of the self-heating of metallic thermometers, discussed in Chapter 4, and the resultant perturbation in the temperature distribution on the calculation of blood flow rate are evaluated. Studies were performed by calculating the steady-state temperature distribution under a range of conditions then setting the power input to zero and recording the temperature decay with time. Unless stated otherwise, the decay rates were measured at 20mm depth in tissue.

5.1.1 The Thermal Clearance Model

The thermal clearance equation may obtained from equation(3.1) where,

$$pc \frac{dT}{dt} = \nabla(k \nabla T) + q\acute{m} + q\acute{a} + wb \cdot cb(Ta-T) \quad ...(5.1)$$

The blood flow may be determined by measuring the change in temperature of an initially steady-state temperature distribution after the power is shut off.

In the past it has generally been held(3), that blood perfusion is the major mechanism for heat elimination in tissue and that thermal conduction provides only a minor contribution for heat removal. Therefore the thermal

conductivity term is neglected and, for reasons explained in Chapter 2, so is the metabolic term $\dot{q}m$.

Thus we have

$$pc \frac{dT}{dt} = wb \cdot cb(Ta-T) \qquad ...(5.2)$$

Where, wb=perfusion rate

cb=blood heat capacity

Ta=arterial blood temperature

Rearranging we obtain

$$\frac{dT}{dt} = \frac{wb \cdot cb}{pc}(Ta-T) \qquad ...(5.3)$$

If we define $w = wb \cdot cb/pc$ and let $\Delta T = T-Ta$ then

$$\frac{dT}{dt} = -w\Delta T \qquad ...(5.4)$$

If w is constant throughout a particular washout then (5.4) yields ΔT explicitly.

$$\Delta T = \Delta To \exp(-w\Delta t) \qquad ...(5.5)$$

Where, ΔT is defined as above, $\Delta To = To-Ta$ and w is referred to as the thermal dilution time constant.

5.2 ASSUMPTIONS

5.2.1 Immediate Equilibrium

The clearance of heat is assumed not to be limited by the time taken for heat to diffuse to the blood vessels. This equilibrium has been shown to exist for Xe133 studies in

various tissues at flows up to 40ml/100g/min.(4) Since the diffusion coefficient of heat is approximately 100 times greater than that of Xenon, this assumption of diffusion equilibrium is justified.

5.2.2 Removal of Heat Only by Blood Flow

Because of the high diffusion coefficient of heat it may also be conducted into surrounding tissues. The diffusion of heat from regions of high temperature to regions of lower temperature will occur producing a more uniform distribution than is implied from the above formulation (Equation(5.5)). This problem is considered in greater detail below.

5.2.3 Constant Blood Flow

Blood flow in skin increases with temperature through a variety of mechanisms (5), (effect of temperature rises on tissue directly, local nervous control, central control via the hypothalamus and the release of chemical vasodilators). In other tissues however, the interactions of such mechanisms do not always produce the same results. While this effect may be of importance during heating, it has been assumed here that the time interval during which thermal clearance is measured is small enough such that no changes in blood flow occur.

5.3 RESULTS AND DISCUSSION

5.3.1 Influence of Thermal Conductivity

A uniform steady-state temperature distribution, infinite in extent, was produced at temperatures of 42, 52 and 62 ^{o}C, by adjusting the power input. The power was then set to zero and the cooling rate measured over a period of one minute. This procedure was repeated for a number of different blood flow rates. The uniform distribution allows the calculation of the time constants for a range of blood flow rates, with conduction effects eliminated.

Figure(5.1) shows that the time constant (w) increases linearly with blood flow. It also shows that the clearance is independent of the temperatures achieved. That is, all three uniform distributions demonstrated the same linear relationship between the blood flow time constant and the blood flow level.

Simulations using nonuniform distributions, thus introducing thermal gradients, were also performed. The change in the time constant with depth, shown in Figure(5.2), illustrates that the apparent or measured thermal clearance may increase or decrease dependent upon the position of the point measured with respect to the gradient. Hence the shape of the initial gradient is important. This can be attributed to thermal conduction of heat, out of regions at high temperatures, increasing the

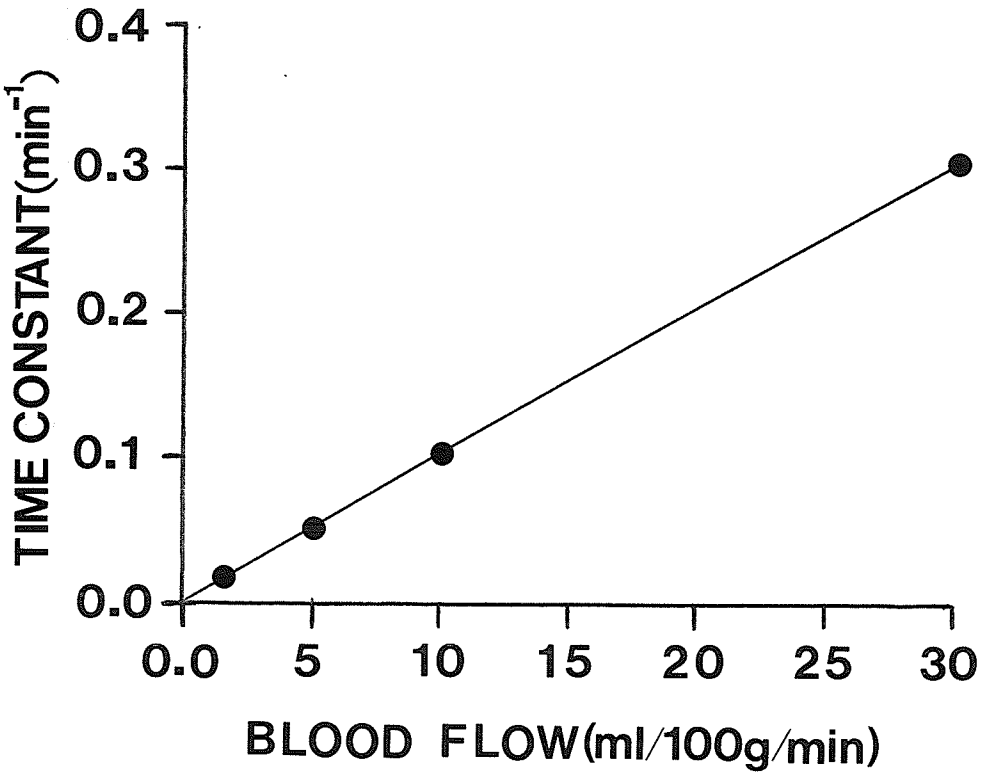

Figure 5.1

The dependence of the thermal clearance time constant on blood flow for uniform temperature distributions.

time constant, or alternatively, to heat conducted into regions at lower temperatures thus lowering the measured clearance rate.

Sandhu(6) also reports that the shape of the temperature decay curve, and hence the time constant measured, is dependent on the temperature distribution at the start of temperature decay. Roemer(7) found similar results and suggested that only "effective" blood perfusion values, which include conductive effects, could be calculated.

It is interesting to note however, that thermal conduction errors may be eliminated even in the presence of temperature gradients. A point of inflection, where $d^2T/dx^2 = 0$, (ie.no net conduction of heat), can be found from the analytical solution given in Chapter 3. Setting the second derivative of the temperature to zero and solving for depth (Appendix B), the point of inflection may be obtained. The results of this calculation agree with the data in Figure(5.2). That is, the point where conduction effects are balanced is the point where the curve intersects the time constant found for a uniform distribution with the same blood flow. (ie/ x=0.963cm) Under the given conditions, this would be the ideal position to measure the thermal clearance rate as the conduction effects would cancel.

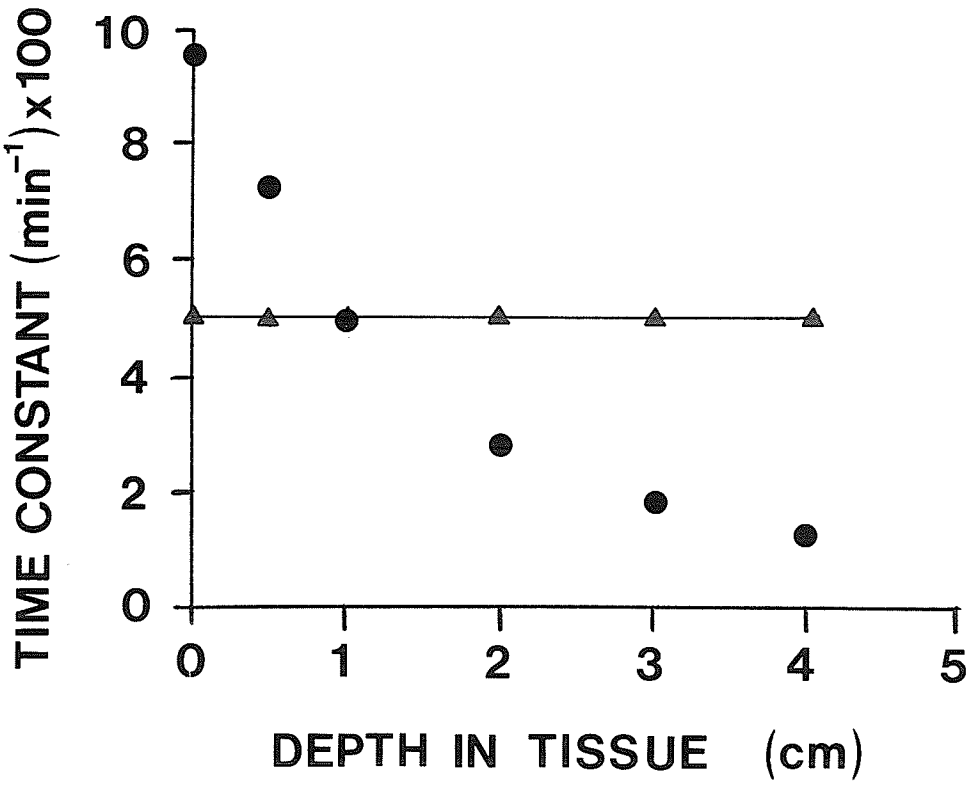

Figure 5.2

The dependence of the blood perfusion time constant on depth in tissue for a,

● Non-uniform distribution
▲ Uniform distribution

Blood perfusion level: 5ml/100g/min.

5.3.2 Influence of Applied Power

As shown above, the thermal gradients present may have a significant effect on the time constant measured. Figure(5.3) shows that in the first 20mm of tissue large changes in the time constant occur with changes in the applied power. As changes in the applied power imply changes in the steady-state temperature distribution, the variations in the time constants measured may again be attributed to conductive effects.

Note from Figure(5.3), that below 20mm depth, the conductive effects appear to be reduced as little change is found in the time constants for the range of initial temperature gradients. The blood flow may therefore be determined with a greater degree of accuracy at these depths. This is further supported by the point of inflection calculated for the different power inputs used. The points cover a range in depth from 1.7 cm to 2.0 cm.

5.3.3 Influence of Surface Cooling

The degree of surface cooling can also affect the accuracy with which the blood flow may be measured. Surface cooling may alter the thermal clearance rate by more than a factor of two as shown in Figure(5.4). The magnitude of the change is not reduced if forced cooling is halted at the power-off time. This implies that the different temperature

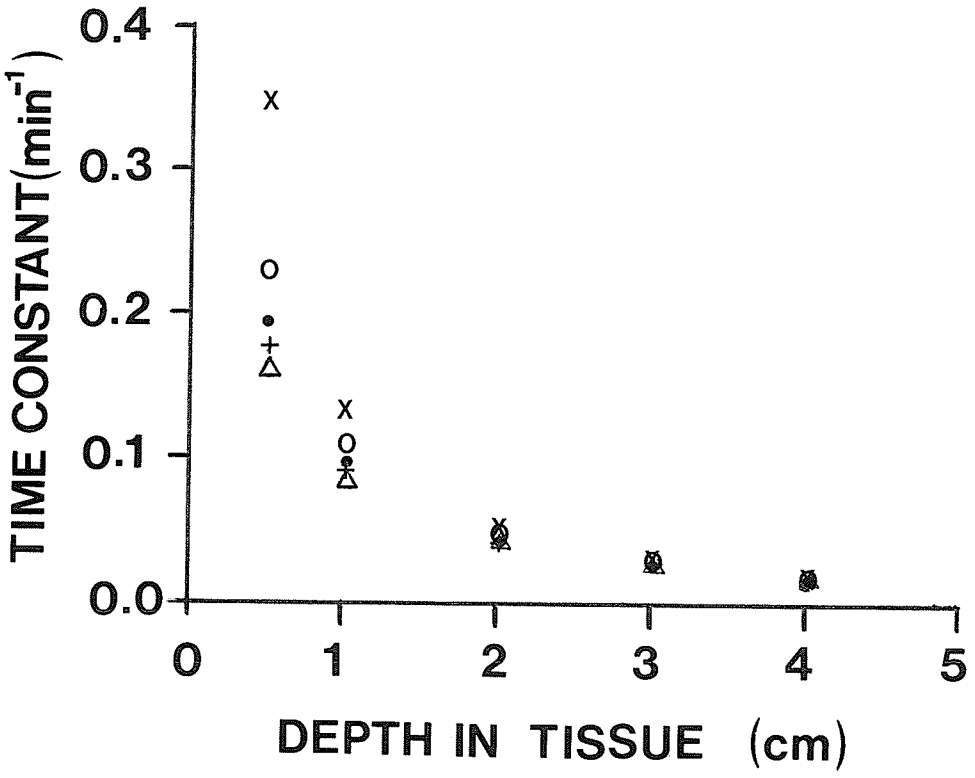

Figure 5.3

The dependence of the thermal clearance time constant on depth in tissue for a range of power inputs. For power densities of

X 2.93×10^5 W/m^3
O 2.51×10^5 W/m^3
• 2.09×10^5 W/m^3
\+ 1.67×10^5 W/m^3
Δ 1.26×10^5 W/m^3

Blood perfusion level: 5ml/100g/min.

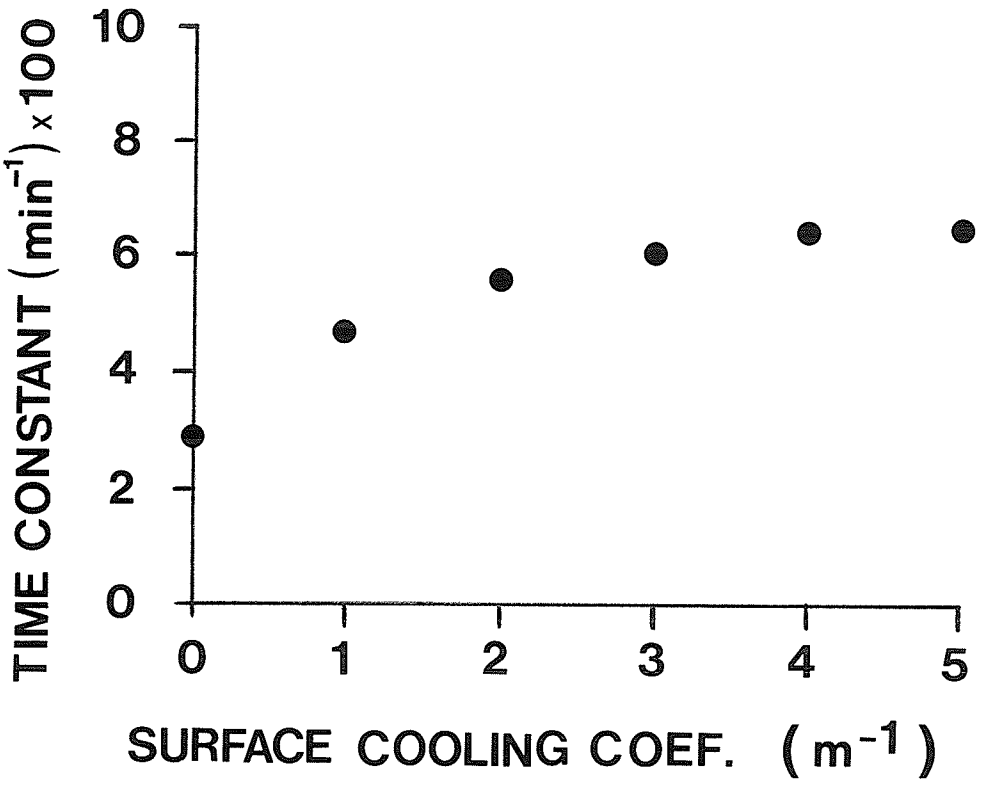

Figure 5.4

The dependence of the thermal clearance time constant on the surface cooling coefficient.

gradients present at the power off time, with different surface cooling and power input coefficients, are responsible for the changes found. Figure(5.4) shows that as the surface cooling increases from 0 to $5m^{-1}$, the calculated time constant changes from first underestimating the clearance rate to overestimating the clearance rate. This change coincides with the changes in the calculated point of inflection which moves from 0.96cm depth, through the 2.0cm mark where the thermal clearance is measured, to 2.3cm depth, as the surface cooling coefficient is increased.

5.3.4 Influence of Thermometer Assembly

The influence of the probe time constant and the temperature perturbation on the measurement of the thermal clearance time constant were also investigated. Studies covering a wide range of thermal properties for the thermometer assembly,(diffusivities of 3.50E-8 to 1.0E-7 m^2 /sec), indicate that the size of the temperature perturbation influences the calculation of the blood flow rate to a greater extent than the actual thermal properties of the probe.

Figures (5.5) and (5.6) show that the thermal properties of the probe have little effect on the time constant measured. The primary factor is the size of the initial temperature perturbation produced by the assembly. With an

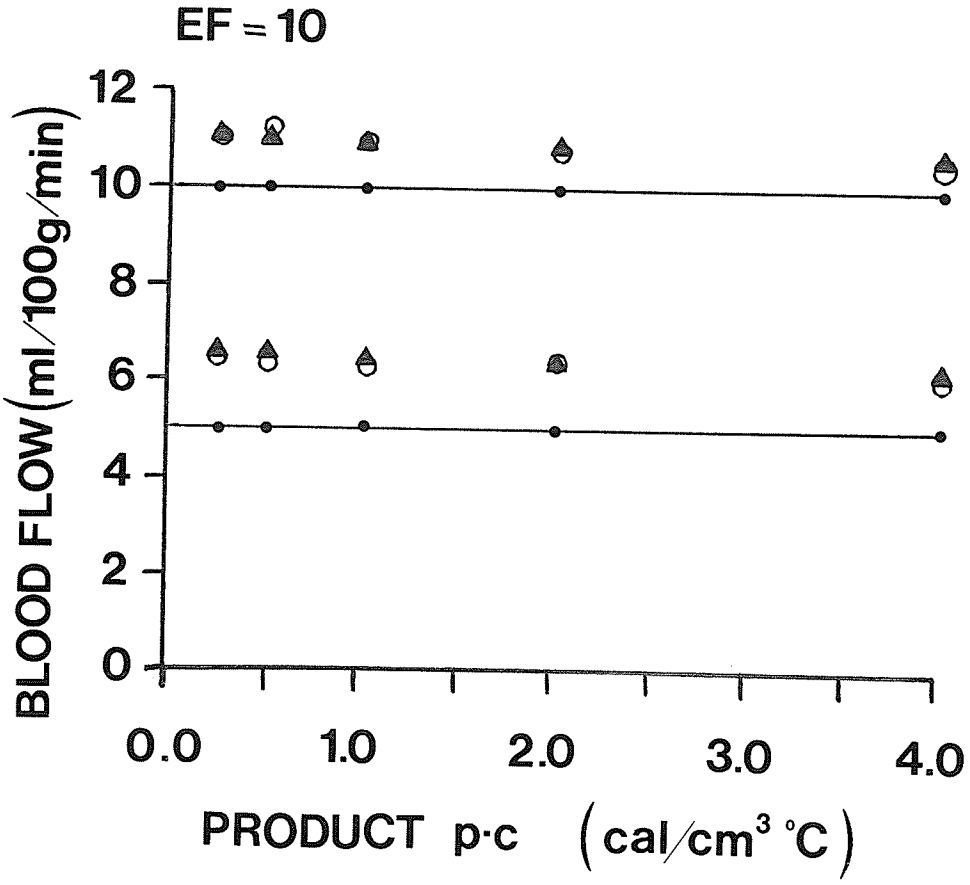

Figure 5.5

The dependence of the blood flow value calculated from thermal clearance on the thermal properties of the probe. (for two blood flow levels)
Diffusivity of probe O 1.0×10^{-3} cm^2/sec
▲ 3.5×10^{-4} cm^2/sec
• actual blood flow level

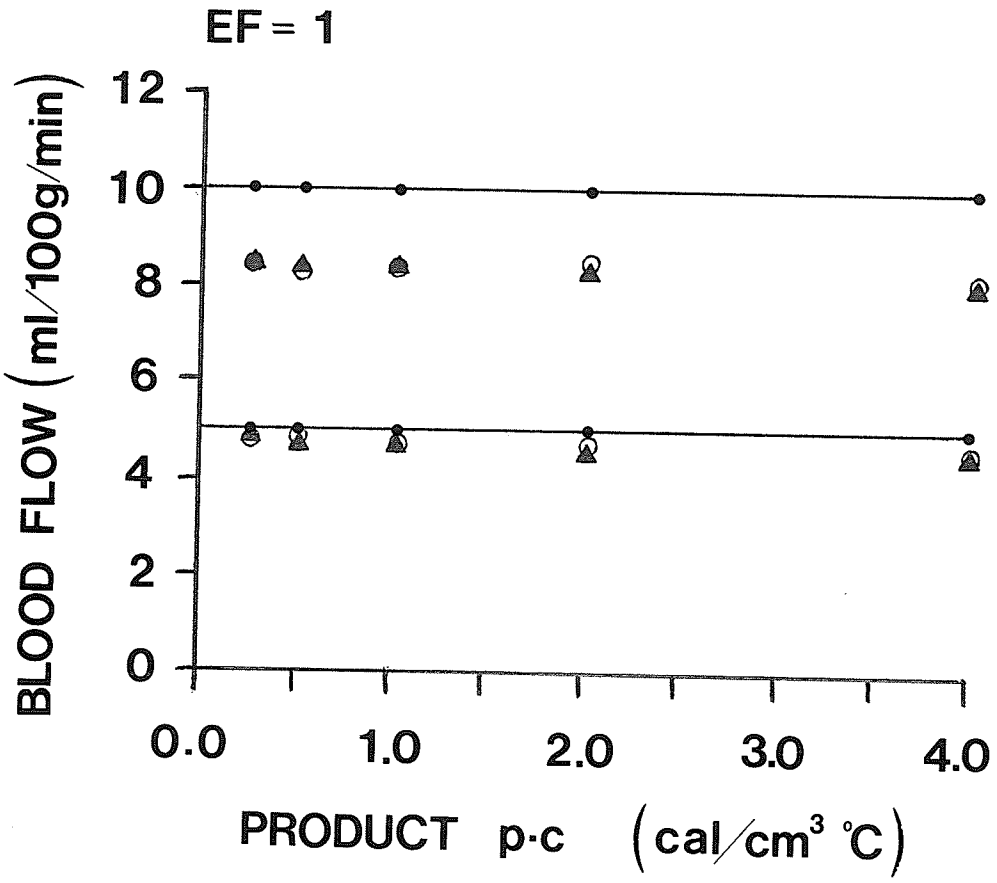

Figure 5.6

The dependence of the blood flow value calculated from thermal clearance on the thermal properties of the probe. (for two blood flow levels)
Diffusivity of probe O 1.0×10^{-3} cm^2/sec
▲ 3.5×10^{-4} cm^2/sec
• actual blood flow level

EF of 10, Figure(5.5) shows that the blood flow level will be overestimated. With this enhancement factor, exaggerated temperature gradients exist in the neighborhood of the assembly at the start of the cooling period. Thus when the power is turned off, the conduction of heat down the temperature gradient, will lead to an overestimation of the actual blood flow.

However, with an enhancement factor of one, the initial temperature gradients will be small. Figure(5.6) shows that with this EF the calculated blood perfusion level is lower than the actual level. Since the only mechanism by which heat may be removed from the probe is thermal conduction, the temperature decay rate of the probe lags behind that of the surrounding tissue thus leading to a lower apparent blood flow value. It is expected that if the diffusivity of the thermometer assembly were high enough the probe would not lag behind the cooling rate of the surrounding tissue. However, for the range of thermal properties covered in this study, the response rate of the probe appears to be insensitive to the diffusivity.

Waterman(8) has shown that with a decrease in the response time of the temperature probe upon insertion into a catheter there is a resultant decrease in the blood flow rate determined using thermal clearance techniques. The results presented here support Waterman's findings but also

indicate that the magnitude of the temperature perturbation, and hence the self-heating effect play a significant role in determining the size of the errors.

5.4 CONCLUSIONS

When using thermal clearance techniques in the determination of blood flow levels, significant errors may be encountered if thermal conduction effects are neglected in the analysis of the temperature decay curves. However, these errors may be eliminated, even in the presence of temperature gradients, if the measurements are taken at the point of inflection. In addition, the thermal properties of the temperature probe and the size of the temperature perturbation in the initial distribution as a result of heating of the probe provide further difficulties when measuring blood perfusion levels.

5.5 REFERENCES

1. Song C.W., Natl. Cancer Inst. Monograph 61,169-176,1982

2. Eberhart R.C., Shitzer A., Ann. NY. Acad. Sci. 335,86-97,1980

3. Milligan A.J., et al, Int. J. Rad. Oncology Biol. Phys. vol.9,1335-1343,1983

4. Patterson J., Strang R., Int. J. Rad. Oncol. Biol. Phys., 9,1335-1334,1983

5. Hertzman A.B., Advances in Biology of Skin. Montagna W., Ellis R.A.,(eds) Pergamon Press, London, 98-116,1961

6. Sandhu T.S., Int. J. Rad. Oncology Biol. Phys. vol.12,1986

7. Roemer R.B., et al, Int. J. Rad. Oncol. Biol. Phys. 11,1539-1550,1985

8. Waterman F.M., Med. Physics, 12(3),368-372,1985

Chapter VI

CONCLUSIONS

The five heat transfer mechanisms which lead to the development of the bioheat equation have been discussed and numerical solutions of the bioheat equation using finite difference techniques presented.

Using the model, the effects of self-heating of metallic thermometers under microwave irradiation were studied. It was observed that the perturbation in the temperature distribution increases with an increase in the enhancement factor and with an increase in blood flow. Increasing the depth at which the thermometer is placed in tissue and increasing the diameter of the assembly both lead to a decrease in the size of the temperature perturbation.

The maximum perturbation likely to be encountered in a clinical setting is 3 ^{o}Celsius. The direct biological effect of this perturbation will be small due to its limited extent. However serious difficulties may be encountered due to the overestimation of the temperature distribution. In addition, clinical trials designed to evaluate the efficacy of a particular treatment regimen will be of limited use if the dosimetry is incorrect due to artifactual temperature measurements.

This increase in tissue temperature in the vicinity of the probe may also have an effect on the determination of blood perfusion levels when using thermal clearance techniques. Either overestimation or underestimation of the perfusion level will occur dependent upon the perfusion level itself and upon the enhancement factor of the probe. However, the errors encountered as a result of the self-heating of the probe are small compared to the errors associated with thermal conduction effects in regions of changing gradients.

Until more accurate and detailed anatomical and physiological information can be readily obtained, the accuracy and usefulness of any thermal model will be limited. The required anatomical information includes a detailed description of tissue structure, including the presence of inhomogeneities, and a detailed description of the vascular bed. Consideration of inhomogeneities would then require a more detailed analysis of the interaction of EM-waves with anatomical structures. The physiological information required must include a desciption of the response of both the tissue and the vasculature to a heat insult.

A more rigorous analysis of the interaction of the EM-field with metallic temperature monitoring devices may allow for the correction of the thermal perturbation

associated with these devices. Furthermore, the continued development of nonperturbing temperature probes and/or noninvasive means of monitoring temperatures may eliminate the need for these perturbing probes. Thus much work remains to be done both in the modelling of the heat transfer mechanisms involved in hyperthermia and on the technology of heat delivery and temperature monitoring systems.

Appendix A

DERIVATION OF THE HOPSCOTCH ALGORITHM

A.1 THEORY

Consider the linear equation shown below

$$\frac{dU}{dt} = LU + g(x,y,t) \qquad \ldots(1.a)$$

where L is a second order linear differential operator and x,y are the spatial variables and t is the time variable. L is defined in detail below.

A solution is required in a closed region R in the x,y plane. Therefore a grid is introduced in the region R, giving a set of points $(ih,jh) \in Rh$ where i,j are integers, m=1,...,M, where t=mk is a plane parallel to R, with k and h the mesh spacings in time and space respectively. If we let uij represent the approximate solution to equation (1.a) at the point (ih,jh,mk) then the exact solution of the differential equation at this point is U(ih,jh,mk). From Gordon (1) we can write

$$u_{ij}^{m+1} = u_{ij}^{m} + k(L u_{ij}^{m} + g_{ij}^{m}) \qquad \ldots(2.a)$$

$$u_{ij}^{m+1} = u_{ij}^{m} + k(L u_{ij}^{m+1} + g_{ij}^{m+1}) \qquad \ldots(3.a)$$

The first step is to evaluate the solution at points (i,j,m+1) using (2.a) for those points where (i+j)=even. Then using equation (3.a) evaluate the solution at those points for which (i+j) is odd. Note: If $L u_{ij}^{m+1}$ is a replacement involving u_{ij}^{m+1} and its nearest neighbors along grid lines ($u_{i+1,j}^{m+1}$, $u_{i-1,j}^{m+1}$, $u_{i,j+1}^{m+1}$, $u_{i,j-1}^{m+1}$) then the algorithm is explicit. At the following time steps the roles of odd and even formulas are interchanged. Therefore equation(2.a) is used where (i+j) is odd and equation(3.a) is used at points with (i+j)even.

We can however replace equations (2.a) and (3.a) by a single equation which defines the algorithm locally at all points. For this we introduce the odd-even function

$$\Theta_{ij} = \begin{cases} 1 & \text{if } m+i+j \text{ odd} \\ 0 & \text{if } m+i+j \text{ even} \end{cases}$$

Therefore we can write the replacement of (1.a) as

$$u_{ij}^{m+1} - k\Theta_{ij}^{m+1} \left[L u_{ij}^{m+1} + g_{ij}^{m+1} \right] = u_{ij}^{m} + k\Theta_{ij}^{m} \left[L u_{ij}^{m} + g_{ij}^{m} \right] \qquad \ldots(4.a)$$

which upon rewriting becomes

$$u_{ij}^{m+1} = u_{ij}^{m} + k\Theta_{ij}^{m} \left[L u_{ij}^{m} + g_{ij}^{m} \right] + k\Theta_{ij}^{m+1} \left[L u_{ij}^{m+1} + g_{ij}^{m+1} \right] \qquad \ldots(5.a)$$

Consider two successive equations of the form (4.a),

$$u_{ij}^{m+1} - k\Theta_{ij}^{m+1}\,[\,L u_{ij}^{m+1} + g_{ij}^{m+1}\,] = u_{ij}^{m} + k\Theta_{ij}^{m}\,[L u_{ij}^{m} + g_{ij}^{m}]$$

...(6.a)

$$u_{ij}^{m+2} - k\Theta_{ij}^{m+2}\,[\,L u_{ij}^{m+2} + g_{ij}^{m+2}\,] = u_{ij}^{m+1} + k\Theta_{ij}^{m+1}\,[L u_{ij}^{m+1} + g_{ij}^{m+1}\,]$$

...(7.a)

From (6.a) we have that

$$k\Theta_{ij}^{m+1}\,[\,L u_{ij}^{m+1} + g_{ij}^{m+1}\,] = u_{ij}^{m+1} - u_{ij}^{m} - k\Theta_{ij}^{m}\,[L u_{ij}^{m} + g_{ij}^{m}]$$

...(8.a)

and, substituting (8.a) into (7.a) we obtain

$$u_{ij}^{m+2} - k\Theta_{ij}^{m+2}\,[\,L u_{ij}^{m+2} + g_{ij}^{m+2}\,] =$$

$$2u_{ij}^{m+1} - (\,u_{ij}^{m} + k\Theta_{ij}^{m}\,[L u_{ij}^{m} + g_{ij}^{m}]) \qquad ...(9.a)$$

Note that for m+1+j an even integer $\Theta_{ij}^{m} = \Theta_{ij}^{m+2} = 0$ and

$$u_{ij}^{m+2} = 2u_{ij}^{m+1} - u_{ij}^{m} \qquad ...(10.a)$$

which allows the definition of a fast Hopscotch algorithm for solution of the bioheat equation as shown below. The algorithm is defined as proceeding from time level t=mk forwards in time.

(1)For interior mesh points , with (m+i+j) an odd integer, the value of T_{ij}^{m} is overwritten with

$$T_{ij}^{m+1} = T_{ij}^{m} + \left| \frac{k\Delta t}{pc}(L T_{ij}^{m}) + \frac{\Delta t}{pc} R_{ij}^{m} \right| \qquad ...(11.a)$$

for all i,j satisfying (m+i+j) odd.

Where LT_{ij}^{m} and R_{ij}^{m} are defined as:

$$LT_{ij}^{m} = [T^{m}(i+1,j)-2T^{m}(i,j)+T^{m}(i-1,j)] + [T^{m}(i,j+1)-2T^{m}(i,j)+T^{m}(i,j-1)] \quad ...(12.a)$$

$$R_{ij}^{m} = H(i,j) - C(i,j,T) \quad ...(13.a)$$

Note: step(1) will only be used if m=mo (starting point) or print-out has been given at t=mk (restart procedure).

(2)If the values of T_{ij}^{m+1} are required for print-out, overwrite the values of T_{ij}^{m} for (m+1+i+j) odd by the equation:

$$T_{ij}^{m+1} - \frac{k\Delta t}{pc}(LT_{ij}^{m+1}) = T_{ij}^{m} + \frac{\Delta t}{pc} R_{ij}^{m+1} \quad ...(14.a)$$

Note: This defines the values of T_{ij}^{m+1} with (m+1+i+j) odd, explicitly if the operator (L) is an E-operator. Since LTij is a replacement which involves Tij and its nearest neighbors along grid lines (Ti+1,j ,Ti-1,j ,Ti,j+1, Ti,j-1) then the algorithm is explicit, and L is refered to as an E-operator. An E-operator can only be a replacement of a 1st or 2nd order differential expression.

After print-out m is incremented by 1 and the calculation returns to step(1).If the values of T_{ij}^{m+1} are not required for print-out proceed to step(3).

(3)For a fixed value of (i,j) with (m+1+i+j) odd, define T_{ij}^{m+1} by

$$T_{ij}^{m+1} = T_{ij}^{m} + \frac{k\Delta t}{pc}(LT_{ij}^{m+1}) + \frac{\Delta t}{pc} R_{ij}^{m+1} \qquad ...(15.a)$$

Notice that the values of $T_{i+/-1,j}^{m+1}$, $T_{i,j+/-1}^{m+1}$ required in this formula have been calculated in step(1). Next, the value of T_{ij}^{m} can be overwritten with T_{ij}^{m+2} defined by

$$T_{ij}^{m+2} = 2T_{ij}^{m+1} - T_{ij}^{m} \qquad ...(16.a)$$

For all allowable (i,j) with (m+1+i+j)odd. Then increment m by 1. If the values of T_{ij}^{m+1} are required for print-out then return to step(2), otherwise return to the start of step (3) and repeat.

The above algorithm does not take into account the redefinition of boundary data but this may easily be incorporated at the start of step(2) or (3). It is also worth noting that the Hopscotch algorithm may be compared to the staggered mesh schemes used in fluid dynamical calculations(3).

A.2 REFERENCES

1. Gordon P., J. Soc. Ind. Appl. Math. 13,667,1965
2. Gourlay A.R., J. Inst. Maths. Applics. 6,375-390,1970
3. Richtmyer R.D., Morton K.W., Difference Methods for Initial Value Problems. Wiley Interscience,1967

Appendix B

CALCULATION OF THE POINT OF INFLECTION

B.1 THEORY

By taking the second derivative of the temperature with respect to depth in Foster's analytical solution(1) and setting this to zero, the point of inflection, where there is no net thermal conduction, can be calculated.

Foster's analytical solution for the 1-D steady-state temperature distribution is written as

$$T(x) = \frac{A/k}{bf-1/L^2}\left| e^{(-x/L)} - \frac{1/L+ \alpha}{\alpha+\sqrt{bf}} e^{(-x\sqrt{bf})}\right| + \frac{\alpha(TA-To)}{\alpha+\sqrt{bf}} e^{(-x\sqrt{bf})} + 37 \qquad ...(1.b)$$

Where the parameters are as defined in Chapter 3.

Letting $A = A/k(bf - 1/L^2)$

$$B = (1/L + \alpha)/(\alpha + \sqrt{bf})$$

$$C = \alpha(TA - To)/(\alpha + \sqrt{bf})$$

we have

$$T(x) = A\left(e^{-x/L} - B\, e^{-x\sqrt{bf}}\right) + C\, e^{-x\sqrt{bf}} \qquad ...(2.b)$$

Taking the first derivative of T(x) with respect to x yields

$$\frac{dT}{dx} = A\left[(-1/L)\, e^{-x/L} - B\,(-\sqrt{bf})\, e^{-x\sqrt{bf}}\right] + C(-\sqrt{bf})\, e^{-x\sqrt{bf}} \qquad ...(3.b)$$

The second derivative is then given by

$$\frac{d^2T}{dx^2} = A\left[(1/L^2)\, e^{-x/L} - B\,(bf)\, e^{-x\sqrt{bf}}\right] + C\,(bf)\, e^{-x\sqrt{bf}} \qquad \ldots(4.b)$$

Setting the second derivative to zero and grouping the x variable terms on the left hand side we obtain

$$e^{x(1/L - \sqrt{bf})} = \left[\frac{A}{(L^2 bf)(AB - C)}\right] \qquad \ldots(5.b)$$

Taking the natural logarithm of both sides and solving for x then yields

$$x = \frac{1}{1/L - \sqrt{bf}} \cdot \ln\left[\frac{A}{L^2\, bf\, (AB - C)}\right] \qquad \ldots(6.b)$$

The depth at which this point occurs in tissue represents the optimum position for measuring the thermal clearance rate. At this depth the conduction effects will be balanced, that is there will be no net heat flow in or out of that point. The thermal clearance measured at that point therefore will depend only on the blood flow at that point.

B.2 REFERENCES

1. Foster K.R., Kritikos H.N., Schwan H.P., IEEE Trans. Biomed. Eng., BME-25(3)313-316,1978